Master's thesis

Robustness of proton treatment plan in patients with left-sided breast cancer treated in deep inspiration breath hold

I.C. (Iris) Huele
MSc Technical Medicine – Imaging and Intervention
Januari 2023

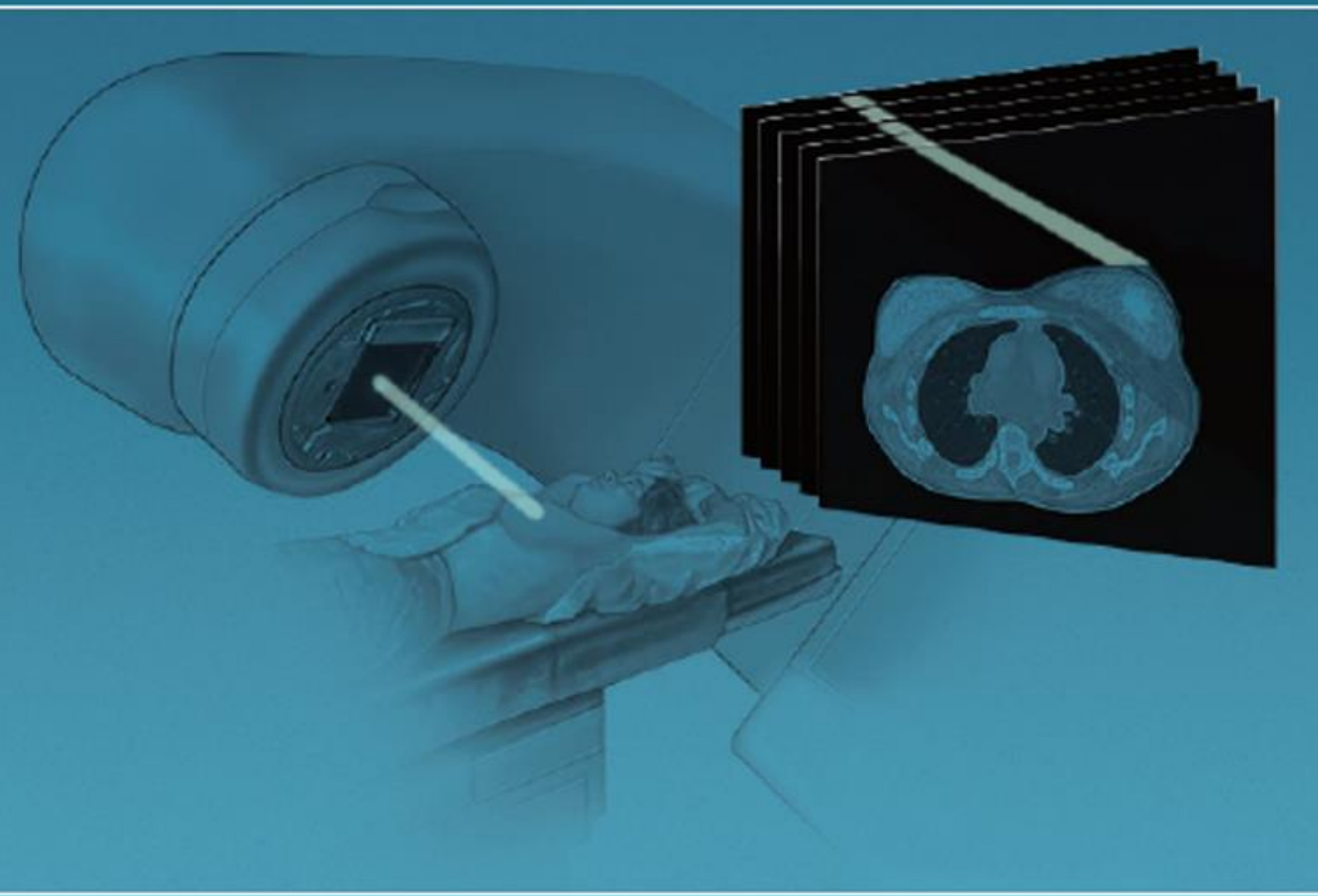

Leids Universitair Medisch Centrum
TU Delft
Erasmus MC

MSc Technical Medicine - Master Thesis

Robustness of proton treatment plans in patients with left-sided breast cancer treated in deep inspiration breath hold

I.C (Iris) Huele
Student number 4488563

Thesis is partial fulfilment of the requirements fro the joint degree of Master of Science in *Technical Medicine*
Leiden University ; Delft University of Technology ; Erasmus University Rotterdam

Master's Thesis project (TM30004 — 35 ETCS)
Department of Radiotherapy, Erasmus MC
Holland PTC
April 2022 - December 2022

Supervision
Dr. J.J. (Joan) Penninkhof, Erasmus MC (Technical Supervisor)
Dr. S.C.J. (Sophie) Bosma, Holland PTC (Medical Supervisor)
Dr. R. (Rob) Louwe, Holland PTC (Technical Supervisor)

Thesis committee members
Prof. dr. M.S. (Mischa) Hoogeman (Chair)
Dr. J.J. (Joan) Penninkhof, Erasmus MC (Technical Supervisor)
Dr. S.C.J. (Sophie) Bosma, Holland PTC (Medical Supervisor)
Dr. R. (Rob) Louwe, Holland PTC (Technical Supervisor)

Leids Universitair Medisch Centrum
TU Delft Delft University of Technology
Erasmus MC Universitair Medisch Centrum Rotterdam

ABSTRACT

Purpose

Deep inspiration breath hold (DIBH) in photon therapy as well as proton therapy (in free breathing) has been suggested to reduce cardiopulmonary and integral dose without compromising target coverage. The goal is to investigate the dosimetric impact on proton treatment plans of set-up variation and daily anatomy visualized on CBCT prior to treatment in patient with left-sided breast cancer patients with an indication for locoregional irradiation.

Method

For 10 patients, proton plans (4.05 Gy in 15 fractions) were made in Erasmus iCycle with a robustness setting of 5 mm and 3% range uncertainties. The CTV included the left breast (n=5) or chestwall (n=5), axillary lymphnodes levels 1-4 and internal mammary chain (IMC).
The daily estimated dose was calculated on five CBCT for proton plans of 10 patients treated for left-sided breast cancer with image guided radiotherapy and surface guidance to facilitate DIBH. A workflow in MIM was created to generate virtual CTs by deforming the pCT into the CBCT.
Dosimetric parameters were evaluated for four separate CTVs; CTV Breast/Chestwall, axillary lymph node levels L1+L2, L3+L4 and left IMC and included the volume, D98, V95 and V107. For OAR this included the volume, Dmean, D2cc and V5Gy for the heart and V5gy and V20Gy for the left lung. To determine whether there was a significant difference between the DVH parameters and volume between the pCT and the mean estimated dose of five fractions a wilxocon signed rank test or two tailed t-test was used. In addition, contour deformation was validated with the Dice similarity score and mean distance to agreement, and it was tested whether there was a significant difference in DVH parameters for CTV chest wall/Breast, CTV L1-L2, and heart between contours derived by the method and contours manually corrected by an experienced breast radiation oncologist on the CBCT.

Results

The mean and standard deviation (std) values observed in this study for the DSC and MDA are 0.98 (0.1) and 0.30 (0.2), respectively, which is in agreement with the proposed tolerances for both evaluation tools. Moreover, no significant difference was found in volume and DVH parameters between the semi-automatic contours derived from the method and the manually corrected contours. A significant difference in volume with a small absolute volume for CTV breast, Chestwall and L1-L2 was observerd and no significant difference in any of the DVH parameters for CTV breast, chestwall, L1-L2, L3-L4 and IMC. The cardiac dose did not have a significant difference in DVH parameters, but the left lung had a significant increase in V5Gy[cc] and V20Gy [cc].

Conclusion

Proton treatment plans created in Erasmus-iCycle on planning CT in DIBH for patients with left-sided breast cancer with indication for irradiation of the breast/chestwall, axillary lymph nodes and IMC achieve good coverage in the mean estimated delivered dose of five fractions treated with image guided radiotherapy and surface guidance for DIBH.

Contents

INTRODUCTION

General introduction

Breast cancer has the highest incidence of all cancer types among women worldwide. In the Netherlands, approximately eighteen thousand women are diagnosed with invasive breast cancer each year.[1] For patients with early-stage breast cancer, treatment consisting of (breast-conserving) surgery followed by radiotherapy to the breast is the standard treatment. In a meta-analysis by the Early Breast Cancer Trialist' Collaborative Group (EBCTCG), radiotherapy after breast-conserving surgery reduced the 10-year risk of any recurrence from 35% to 19.3% and an absolute reduction in 15-year mortality of 3.8% was reported.[2] In addition, radiotherapy to the chestwall (with/without regional lymph nodes) after a mastectomy is recommended in patients with high-risk disease.

However, for patients with left-sided breast cancer treated with radiotherapy, particulary to the internal mammary lymph nodes, radiation-induced cardiac mortality might partially offset this breast cancer-specific survival advantage.[3,4] Darby et al[5] showed that the rate of major coronary events increases linearly with 7.4% per Gy in the mean heart dose, or even higher in patients with preexisting cardiac risk factors. This was validated in a dutch cohort with 910 patients.[6] Several heart-sparing techniques have been developed to minimize irradiated heart volumes without compromising the target volume, such as methods of patient positioning, proton therapy and Deep inspirational breath hold (DIBH).[7]

The use of deep inspiration breast hold (DIBH) in radiotherapy for left-sided breast cancer has been proven to reduce the cardiac dose and is widely implemented. This technique physically separates cardiac structures away from the radiation target volume and thereby helps reduce cardiac dose.[8] Also proton therapy reduces the cardiac exposure and due to the model-based inidcation approach used in the Netherlands, proton therapy will mostly be provided to breast cancer patients with lymph node involvement.[9] In proton therapy unlike with photon radiation in VMAT, the absorption of proton radiation has a peak close to the depth rand of the beam, the so-called Bragg peak. The location of the peak is determined by the energy of the proton radiation, and a spread-out Bragg peak can be produced by superimposing multiple energy layers. This is called intensity modulated proton therapy (IMPT) and makes it possible to conform the beam to the clinical target volume in the depth-direction of the beam, but also makes the treatment more sensitive to patient set-up variation.

Positioning errors in radiotherapy with Deep inspiration breath hold (DIBH)

High accuracy is a prerequisite for safe clinical application of radiotherapy. The total radiotherapy treatment consist of multiple fractions, in the Netherlands a treatment consisting of 40.05 Gy over 15 fractions (without simulations integrated boost) is often recommended. The set-up accuracy and organ motion both contribute to the overall treatment accuracy. Ideally, the patient position during pCT is reproduced at each treatment fraction. Deep inspiration breath hold and image-guided radiation therapy are two developments that could assist in reducing inter- and intra- fraction variation. DIBH has shown to reduce the respiratory motion during dose delivery.[8] Image-guided radiation therapy (IGRT) can be used to image the patient in treatment position immediately prior to treatment delivery. IGRT has been proven to improve patient positioning and minimize the setup error.[10]

Modalities such as electronic portal imaging devices, cone beam CT (CBCT) and surface imaging have been implemented to verify the setup accuracy in both 2D and 3D view of patients with left-sided breast cancer treatment. For example, a CBCT image is taken pre-treatment but after patient positioning and based on the registration between the CBCT and the pCT, the patient may be shifted to ensure proper positioning prior to treatment. This is called an online protocol, when immediate correction of patient set-up error occurs. In the Netherlands another widely implemented technique is surface-guided radiotherapy (SGRT). SGRT for breast radiotherapy has demonstrated benefits for patient placement, patient monitoring during treatment fractions, gating in free breathing or DIBH, and identifying anatomical alterations over the course of treatment. High spatial and temporal resolution images of the patient's skin location are provided by optical surface scanners. Surface-guided correction of the patient posture, arm and chin position also improves the position of the breast in general.

Despite the reduction of patient positioning variation with IGRT and SGRT, errors still exist between fractions and within fractions. Inter-fraction variation is the variation seen between fractions seen between images taken on different treatment fractions. These variations are commonly quantified as random and systematic errors using group statistics.[11] For an individual patient, the systematic error is the average variation in treatment position compared to their pCT. It is calculated from all treatment verification images across a course of radiation therapy for a particular patient. The random error is the variability in patient positioning between daily treatment verification images, varying in direction and magnitude each day.

Intra-fraction variation is the variability in in positios as can be observed on images acquired during treatment. For example, multiple DIBHs are required to ensure dose delivery within one fraction. The reproducibility of DIBH, the ability to perform the exact same DIBH each breath hold, can influence the intrafraction variation.

Deformed CT

In modern IGRT, CBCT images play an important role in accurate patient position verification and, additionally facilitates the visualization of daily anatomical variations.[12] Daily anatomical changes may influence target coverage and OAR sparing and thereby affect treatment outcome. CBCT can also allow dose verification by calculating the 'dose of the day' and confirming whether the current plan is still suffices for the variation of that day. A prerequisite for dose verification is that the HU calibration's quality is sufficient to enable dose calculation.

However, dose calculation on CBCTs are prone to errors as CBCT possesses image artifacts due to detector scatter, patient specific scatter, image lag and beam hardening.[13]In addition, the imaging volume of the CBCT is limited to the field of view (FOV), as well as being limited in the superior and inferior directions due to the physical dimensions of the EPIDS resulting in limitations in scan length. The relevant ROI includes the left breast and the axillary lymph nodes. Due to the limited FOV the right breast, right lung and often the left-lateral side of the heart are excluded, challenging dose calculation as the planned dose calculated on the pCT includes more anatomical information. A number of studies has recently emerged proposing to correct CBCT imaging artefacts, increase image intensity consistency and expand the FOV with deformable imaging registration (DIR) of the planning CT to the daily anatomy on CBCT.[14–16] Due to these methods an approximation of the delivered dose in the fractions can be calculated.

Goals and objectives

The aim of this thesis is to evaluate the dosimetric impact of daily variations in patient positioning and anatomical changes during treatment. In a dosimetric study the daily dose is calculated on pretreatment CBCT images for proton plans for 10 patients treated for left-sided breast cancer with IGRT and surface guidance to facilitate DIBH to the breast/chestwall, axillary lymph nodes levels 1-4 and internal mammary chain (IMC). The goal is to investigate if proton plans are robust to account for daily position variations by comparing the mean estimated dose as delivered during five fractions with the planned dose on the planning CT assuming online positioning corrections.

MATERIALS AND METHODS

Patient data

For this study, the planning CT and CBCT images of ten patients treated with radiotherapy for left-sided breast cancer in DIBH at the Erasmus MC were used. Five patients were treated with radiotherapy after breast-conserving treatment and five patients received post mastectomy radiotherapy. Prior to treatment, a computed tomography scan (CT, Siemens) with a 3-mm slice thickness of the upper body without intravenous contrast was carried out in DIBH. Patient immobilization (supine) was achieved using a breast board with head holder and both arms lifted above the head. At the treatment unit (Elekta AB, Stockholm, Sweden) SGRT was used for initial positioning both in free breathing (at mid-patient reference point) and in DIBH, after which a relative couch shift was applied to

obtain the treatment isocenter in DIBH. Patient positioning was daily verified and corrected before delivery of the actual treatment beams by using a 180 degree CBCT acquisition in DICH (CBCT, XVI, Elekta AB, Stockholm, Sweden) and registration on the thoracic wall and breast contour. For every patient and fraction, a CBCT pretreatment was available, if multiple CBCTs were available in a fraction, the last CBCT prior to treatment was chosen.

Delineations

Clinical target volumes (CTVs), including breast (CTV breast) or chest wall (CTV chestwall), axillary lymph node levels 1-2 (CTV L1+L2), axillary lymph nodes level 3-4 (CTV L3+L4) and left IMN (CTV IMC), were delineated in MIM (MIM Software Inc., version 7.1.6, Cleveland, OH) according to ESTRO guidelines.[17] The CTV breast was cropped 5 mm from the skin. All CTVs were combined in CTV Total. Delineations of CTVs and organs at risk (OARs) were supervised by a breast radiation oncologist. The OAR structures included the contra-lateral breast, left lung, right lung, skin and the heart. Delineation of the heart was performed according to Feng et al.[18]

Deformed CT

A workflow was created to generate a synthetic CT for dose calculation. The deformed CT represents the daily anatomy of the CBCT with the HU window to facilitate calculation and evaluation of the dose delivered during treatment. This workflow consisted of sub-workflows applied sequentially in the software MIM, as shown in Fig 1 and describe below (additional information can be found in Appendix I DIR specifications).

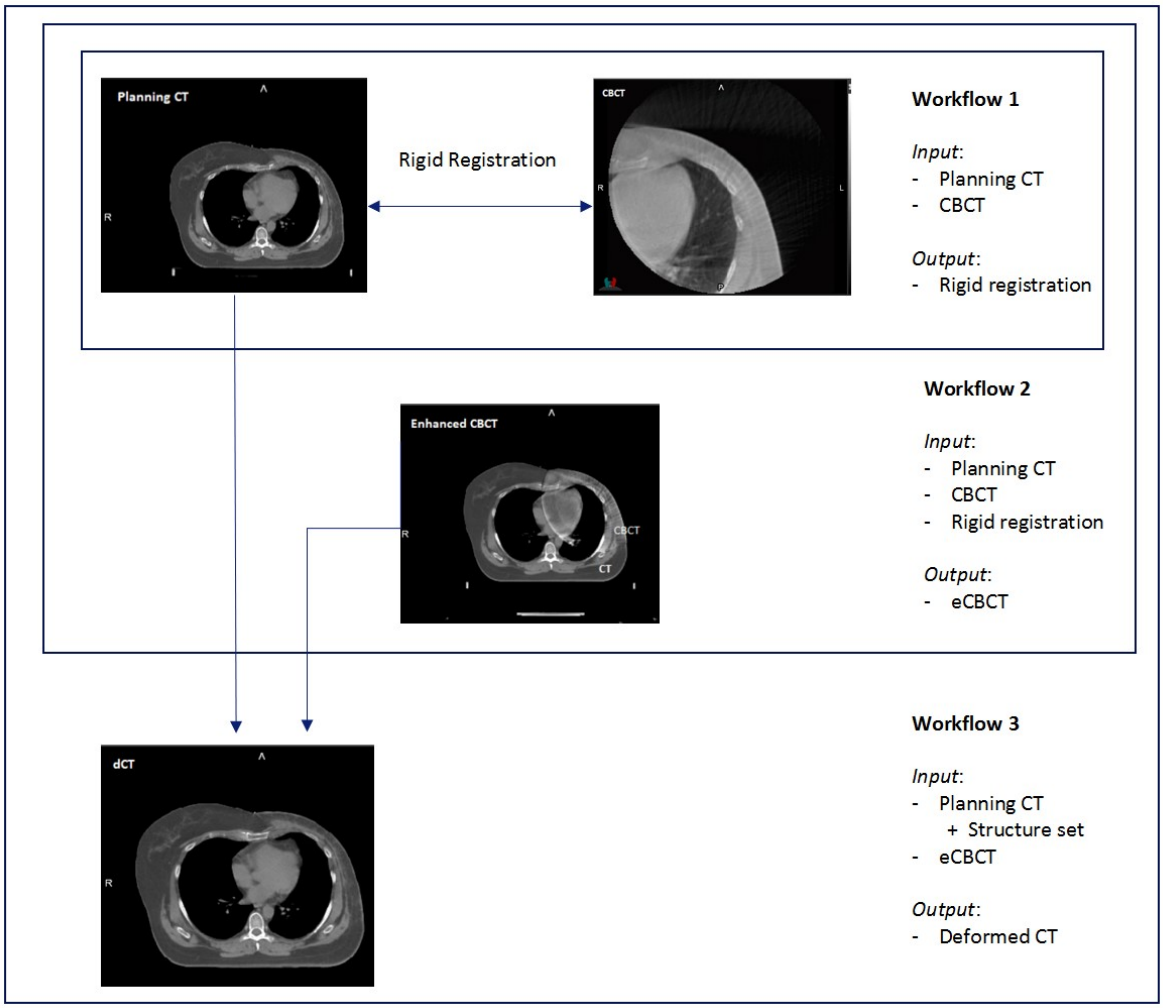

Figure 1: Overview workflow

In step 1, the planning CT and the selected CBCT were registered with a rigid transformation and the rigid transformation was saved. A rigid registration can be applied either to the entire image or to a specific region of interest. In this study, a region of interest (ROI) was registered encompassing the entire breast/ chest wall (figure 2), with all voxels within the box used with equal weighting. This corresponds to the ROI, which was used in the clinical registration procedure prior to treatment. After registration the pCT and CBCT were set in the same frame of reference.

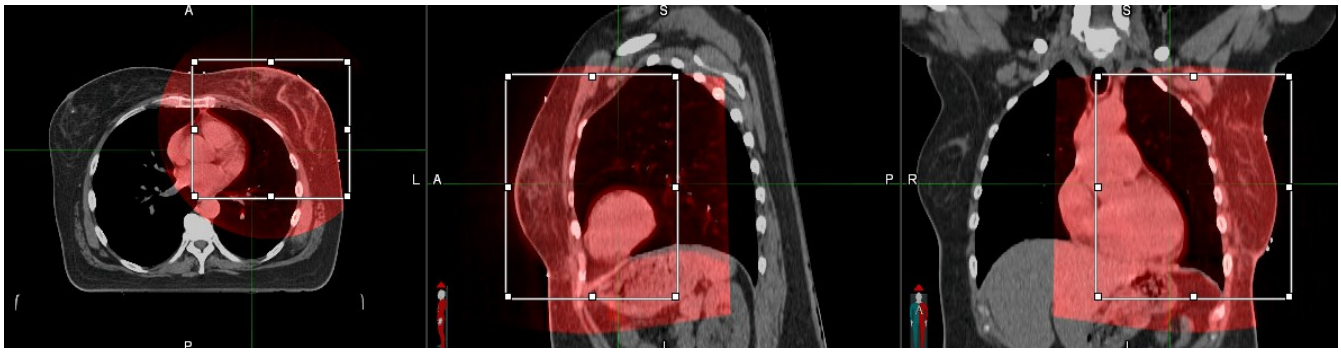

Figure 2: Axial, sagittal and coronal view of the ROI including the entire left sided breast/chestwall for the box-based alignment. pCT (grey), CBCT (red).

In step 2, an enhanced CBCT was created using the MIM Software. In this workflow, three substeps were performed to overcome the shortcomings of the CBCT as descibed above. First, a free-form deformable image registration (DIR) was performed between the CBCT and the pCT, which serves as the basis for the improvement process. In the second step, an enhanced CBCT was created by reducing shading artefacts and improving the CBCT intensity values. In the third part of the workflow, the FOV of the enhanced CBCT was expanded by merging the pCT and enhanced CBCT without deforming the anatomy within CBCT FOV. The output appears as a stitching result consisting of the enhanced CBCT within the FOV of the original CBCT and the deformed pCT outside the original FOV of the CBCT. The deformation of the pCT is continued from the CBCT to the edge of the pCT FOV, rsulting in an enhanced CBCT with improved HU units. However, the remaining difference in HU units compared to the planning CT still makes the enhanced CBCT unsuitable for accurate dose calculation. Appendix I Imperfections eCBCT shows an example of shortcomings on the eCBCT and illustrates the need for a final step in the workflow.

In step 3, the final workflow is applied to create a deformed planning CT. In this workflow, both images, pCT and eCBCT, were masked to perform only the deformable image registration within the patient, thereby excluding any remaining shading artefacts on the eCBCT. The patient contour was obtained from the rigidly transferred pCT contour and several morphological operations. These operations included expanding the pCT contour by 5 mm, performing an interlock to exclude all voxels with HU below -300), removing this interlock, filling holes and a morphological closing with 0.5 cm. The masked pCT was morphed into the CBCT using a free-form deformation (Multi-modality DIR in MIM. This results in a deformed pCT and was saved as dCT for the specified fraction. This workflow also includes the deformation of the structure set of the pCT. The structure set was then subjected to the exact same deformation vector field created during the deformable image registration between the pCT and eCBCT. Fig 14 shows the final dCT with the associated structure set.

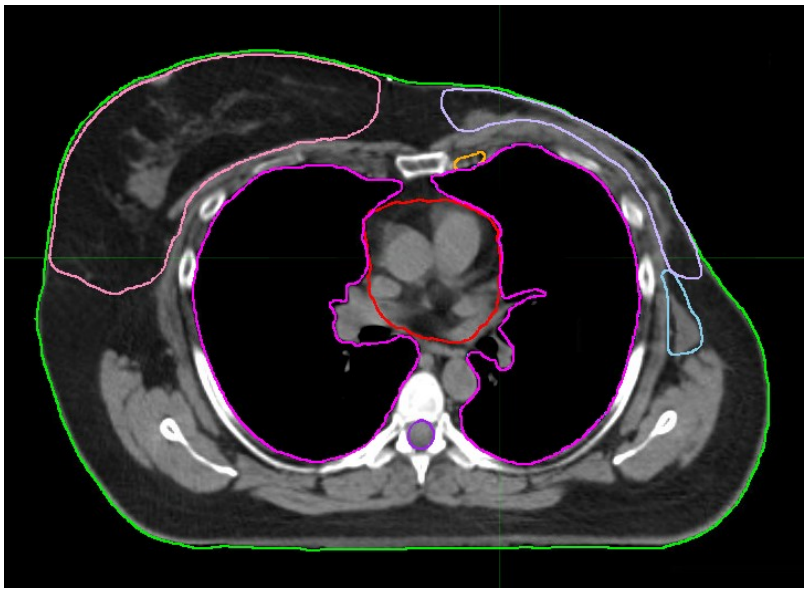

Figure 3: Example for of dCT of one fraction of one patient

MIM contour deformation validation

The accuracy of DIR for an individual patient is difficult to assess because of the lack of a ground truth, which makes the development of standardized means to evaluate the results of a DIR technique challenging. Besides a visual inspection of the dCT, validation of the accuracy of DIR was performed by comparing deformed structures with structures corrected on the eCBCT by an experienced radiation oncologist. The validation was based on a subset of five patients with three randomly selected fractions per patient. CTV breast/CTV chestwall, CTV L1+L2 and heart (only considered if the heart was fully visible on the CBCT) on the eCBCT were manually adjusted by an experienced radiation oncologist based on the visible daily anatomy of the CBCT and were saved as reference contours for validation of the accuracy of DIR. Contour propagation and validation against ground truth contours have been used in both monomodal and multimodal imaging of many anatomical sites, with emphasis on the thoracic-abdominal region.[19,20] The similarity measures were evaluated using the Dice similarity coefficient (DSC), and mean Distance to Agreement (MDA). The Dice similarity coefficient is used to evaluate how similar two objects are, in this case volumes of the compared contours. The dice coefficient can range from 0 to 1, 1 indicates that the objects are identical.[21] MDA compares the mean surface distance between two contours on registered images.[22] The report of the American Association of Physicists in Medicine (AAPM) Task Group No. 132 published in 2017 reviewed rigid image registration and deformable image registration approaches and solutions to provide recommendation for quality assurance and quality control of clinical image registration and fusion techniques in radiotherapy. The reported tolerances for the contour deformation for the evaluation tools are >0.80-0.90 for DSC and <2-3 mm for MDA. In addition, the deformed contours were also validated by evaluating the impact on the dose volume histogram (DVH) parameters. By comparing the contours derived with the semi-automatic workflow with the contours corrected on the eCBCT by a experienced breast radiation oncologist.

Proton plans

For each patient, an intensity modulated proton treatment (IMPT) plan with a prescribed dose (PD) of 40.05 Gy in 15 fractions with robust optimization was created in Erasmus-iCycle.[23]The objectives for proton plans can be seen in Table 1. The most important goals were to cover at least 98% of CTV volume by 95% of the prescribed dose (V95[%]>98%), while preferably keeping the volume receiving 107% of the prescribed dose below 2% (V107[%]<2%). Erasmus-iCycle performs multi-criteria optimization based on a so-called wish-list. In this wish-list, the clinical goals for the CTVs are set as constraints and the clinical goals for OAR as prioritized objectives. These constraints are never violated, while the objectives are optimized one at a time in accordance to their priority. In this way,

pareto-optimal plans are created taking into account the objectives in the wish-list, where a optimal trade-off between conflicting objectives was created.[23] In this study, two wish-lists were created based on the protocol for left-sided breast cancer proton therapy in Holland PTC (Appendix I I-cycle Wishlist). Both wish-lists were created to meet clinical goals for patients (Table 1). The first wish list was created for patients who had undergone mastectomy, and the second wish list was created for patients with breast tissue including an additional goal to minimize dose to the skin. Skin-03 was defined as a Boolean CTV with an extension of 10 mm and an inner ring of 3 mm around the patient contour. The treatment isocenter was defined as the centroid of the CTV total.

Table 1: Clinical goals for Proton treatment plan for patients with left-sided breast cancer. Voxmin is the minimal dose received from the 19 scenarios. Voxmax is the maximal dose receive from the 19 scenarios. Nominal is the dose received from the nominal treatment plan.

Dose	Structure	Dosimetric parameter	Clinical goal
Voxmin	CTV Chestwall/Breast	V95%	98% >(38,05 Gy)
	CTV L1+L4	V95%	98% >(38,05 Gy)
	CTV IMC	V95%	98% >(38,05 Gy)
Voxmax	CTV Total	V107%	2% <(42,85)
Nominal	Heart	Mean	<2,0 Gy
	Lungs	Mean	<7,0 Gy
	Breast contralateral	Mean	<2,0 Gy

To account for inter-fractional- and intra-fractional variations, treatment plans were robustly optimized with an isotropic setup error of 5 mm and a range 3% uncertainty according to local guidelines. The systematic range underestimation arises from the conversion from the CT value to the proton stopping power using a Hounsfield look-up table. This method can not sufficiently deal with different tissues and inter-patient variability. The Paul Scherrer Institute in Switzerland physiologically calibrated its CT scanner to have an accuracy of 1% for soft tissue and 2% for bony tissue; however, because of inherent errors such as beam hardening, reconstruction artifacts, and reconstruction algorithms, it has been argued that an error in HU value of 3% is more realistic.[24,25] Five millimeters set up robustness was assumed to account for geometric errors. The robustness optimization included 19 scenarios: one nominal plan, six cardinal isocenter shifts (5mm) combined with a range -3%, 0% or 3%. Additional optimization parameters are listed in the appendix 14 Robustness analysis involved calculating the dose for treatment scenarios.[26] For the robustness evaluations, the same scenarios were used for optimization. From these 19 scenarios, the voxel-wise maximum and voxel-wise minimum dose distributions were derived by selecting the minimum and maximum dose values from these scenarios for each voxel in these 19 scenarios. CTV coverage was assessed using the voxel-wise minimum dose (voxmin dose) and V107% was assessed using the voxel-wise maximum dose (voxmax dose). The final optimized treatment plans were scaled after evaluation to maximize OAR sparing and reduce V107% in CTVs, while remaining the target coverage of D98 >95% of the PD (38.05 [Gy]). The scale factor was calculated as the largest scale factor (closest to 1) of all separate CTVs to achieve the clinical goals for V95 and D98.

Dosimetric evaluation

For each patient, five deformed CT were created using CBCT images of fractions 1, 4, 8, 12, and 15. These fractions were selected to provide a representative estimate of daily anatomy changes throughout the course of treatment. The dCT was imported into Erasmus iCycle and the original optimized treatment plan from the pCT was calculated on the dCT with the same beam delivery configuration. The mean dose distribution for five fractions were estimated to determine if proton treatment plans with robustness setting (5mm,3%) accounted for geometric errors and range errors. The dCT represents the patient positioning and the daily anatomy of the patient prior to treatment and thus represents the inter fractional variation. However, the remaining intra fractional variation has not been accounted for in the dCT. Therefore, a dose calculation was performed using a robustness recipe of 1mm isotropic and 3% range uncertainty. The range uncertainties and geometric uncertainties included in the robustness evaluation of the estimated treatment dose are listed in Table 2. The isotropic error of 1 mm was applied on the summed dose distribution of all three beams. In addition the analysis was also performed using a robustness recipe

of 3mm isotropic and 3% range uncertainty.

Table 2: Range and geometric uncertainties included in the robustness evaluation of the estimated treatment dose

Range uncertainties(%)						
Stopping power prediction[24]	3%					
Geometric uncertainties (mm)	**Systematic + 1 S.D.**			Random + 1 S.D.		
	LR	AP	CC	LR	AP	CC
CT isocenter[27]	± 0.5	± 0.5	± 0.5			
Gantry isocenter[27]				± 0.5	± 0.5	± 0.5
proton beam isocenter	<0.5	<0.5	<0.5	<0.5	<0.5	<0.5
Couch[27]				± 0.2	± 0.2	± 0.2
Online matching[27]				± 0.5	± 0.5	± 0.5
Intra-fraction[28,29]	± 0.4	± 0.4	± 0.4	± 0.7	± 1.3-1.4	± 1.20
Total uncertanty	**0.92**	**0.92**	**0.92**	**1.01**	**1.58**	**1.40**

Analysis

The planned dose was compared with the estimated delivered dose with respect to the DVH-parameters listed in Table 3. A statistical test was performed to determine whether there was a significant difference between the planned dose on the pCT and the mean estimated delivered dose of five fractions for the DVH-parameters and volumes. First, the Shapiro-Wilk test was used to determine if a sample of data was from a normally distributed population. If the p-value was below the significance level of 0.01, the null hypothesis that the data are normally distributed was rejected and the alternative hypothesis that the data are not normally distributed was accepted. In this case, a non-parametric statistical test, Wilcoxon signed rank test, was used. If the data were normally distributed, a two-tailed t-test was performed. Statistical tests were performed for both robustness settings (1mm,5%) and (3mm,5%).

Table 3: The parameters which are used for the estimated dose evaluation and the number of patients included in the evaluation

CTV - Breast / Chestwall	N	CTV - L1+L2 / L1+L3 / IMC	N	OAR- Heart		OAR- Lung	
Volume [cc]	5	Volume [cc]	10	Volume [cc]	7	V5Gy [cc]	10
D98 [Gy]	5	D98 [Gy]	10	Dmean [Gy]	7	V20Gy [cc]	10
V95 [%]	5	V95 [%]	10	D2cc [Gy]	10		
V107 [%]	5	V107 [%]	10	V5Gy [cc]	10		

RESULTS

MIM contour deformation validation

The mean and standard deviation (std) values observed in this study for the DSC and MDA are 0.98 (0.1) and 0.30 (0.2), respectively, which is in agreement with the proposed tolerances for both evaluation tools. In four of five patients, the heart was fully visualized on the CBCT, therefore one patient was excluded from this subanalysis. Table 4 lists the difference in volumes between the deformed contours and manually delineated contours and mean values for the coverage of CTVs (D98 and V95) and nominal dose to the heart (Dmean and D2cc). The results show that the contours obtained by a breast radiation oncologist were very similar to the contours obtained with the DIR method as none of the differences were statistically significant. The adjustments to the contours were often minor adjustments to the edge of the contour as visualized in figure4. For the CTV, the difference in delineation causes a main difference of 0.6 Gy and 0.6% for the D98 and V95 as can be seen Table 12. For the heart, minor adjustments were often made on the anterior edge, as a consequence, the mean heart dose and D2cc increased. However, No systematic error in contour deformation was observer as none of the difference are significant.

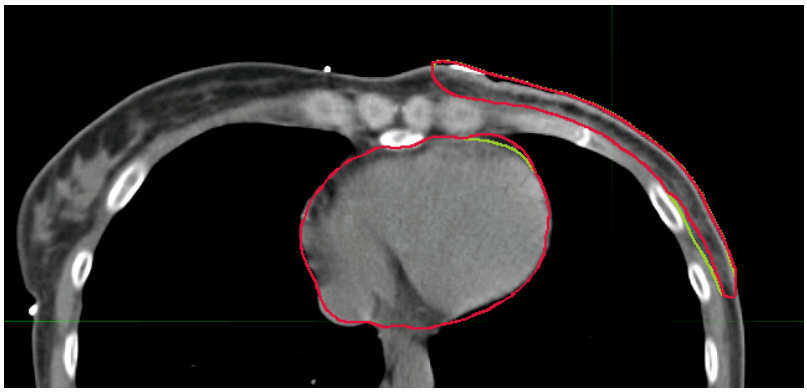

Figure 4: Difference in contours created using either a semi-automatic workflow (green) or these contours manually corrected on the eCBCT a experienced breast radiation oncologist (red)

*Table 4: difference in volume / DVH parameters and significance between the contours created with the semi-automatic method and the contour manually corrected by a experienced breast radiation oncologist. *Mean is the mean value of the semi-automatic method contours.*

CTV	**Volume [cc]**		**D98 [Gy]**			**V95 [%]**		
	$\triangle[min-max]$	p-value	Mean*	$\triangle[min-max]$	p-value	Mean*	$\triangle[min-max]$	p-value
Breast/Breast	-0,01 [-0,02;0,08]	0.77	38.44	-0,63 [-2.95;0,38]	0.08	98.60	-0,64 [-2.85;1,17]	0.18
L1+L2	-0,00 [-0,03;0,03]	0.10	38.39	-0,21 [-0.09;2,98]	0.32	98.45	-0,18 [-0.24;2,14]	0.80
OAR	**Volume [cc]**		**Dmean [Gy]**			**D2cc [Gy]**		
Heart	$\triangle[min-max]$	p-value	Mean*	$\triangle[min-max]$	p-value	Mean*	$\triangle[min-max]$	
	-0,02 [0,00;0,07]	0.25	0.45	-0,07 [-0,01;0,16]	0.68	15.23	-2.54 [0,00;7,25]	0.37

Proton plans

For all 10 patients, treatment plans were made using the general wish lists (Table 13). Figure 5 shows an representative example of an optimized proton plan. The proton plans of all patients, except patient 2 and 3 met the clinical goals stated in the method section. Patient 2 and 44 did not meet the clinical goal of V95% >98% for the CTV IMC, but achieved V95>97,5%. All proton plans met the clinical goals for OARS heart, lungs, and contralateral breast with a mean (std) of 0.41(0.22) 2.59(0.63)Gy, 0.00(0.00)Gy, respectively.

Figure 5: an optimized proton plan for a patient with CTV breast

Dosimetric evaluation Proton plans

The results for the volume and DVH parameters with robustness settings (1mm,3%) are presented in this section. For the robustness setting (3mm,3%) the mean estimated dose in five fractions is presented in the figures and the additional results for each patient are presented in Supplementary Tables Table 15 and Supplementary Figures

section 3mm Robustness Analysis. These results show an significant decrease in DVH parameter V95 [%] of 1.13 [0.02; 5.76] and 3.00 [-0.63;9.25] for CTV L1-L2 and L3-L4, respectively.

CTV Breast

The results of the robust evaluation of the CTV breast (n=5) can be seen in figure 6 and table 5. The volume of the CTV Breast decreased significantly with a mean difference of 39.48 cc. No significant difference between the planned dose and mean estimated dose of the five fractions for any of the DVH parameters was observed. Figure 6d shows that the estimated dose in the five fractions is decreases with an average of 1,5 Gy.

*Table 5: The results for the volume and DVH parameters (D98, V95 and V107) of the CTV Breast in five patients after lumpectomy for pCT, dCT and difference including the associated significance *significant*

Dosimetric Parameter	**pCT mean (std)**	**dCT mean (std)**	**△ mean [range]**	**p-value**	test
Volume [cc]	939.40 (381.87)	903.08 (335.78)	39.48 [-9.18; 107.78]	0.01*	t-test
D98 [Gy]	39.11 (0.14)	38.97 (0.17)	-0.20 [-0.33; 0.40]	0.12	wilcoxon signed rank test
V95 [%]	99.92 (0.04)	99.97 (0.05)	0.01 [-0.33; 0.40]	0.75	wilcoxon signed rank test
V107	0.49 (0.85)	0.05 (0.08)	0.44 [0.00; 1.79]	0.12	wilcoxon signed rank test

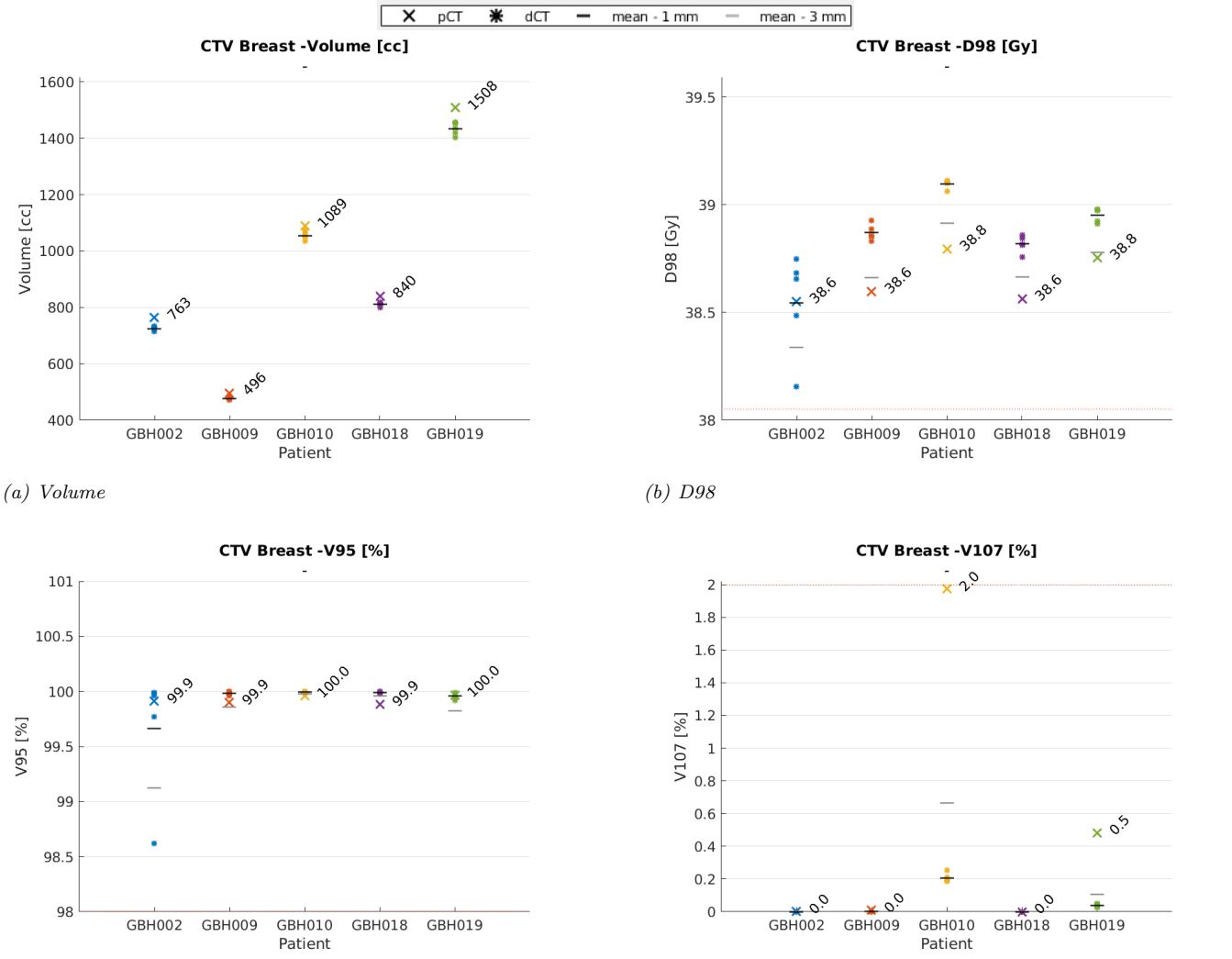

(a) Volume

(b) D98

(c) V95

(d) V107

Figure 6: Robustness evaluation of the volume, D98%, V95% and V107% for the CTV Breast. Panel a visualises the absolute volume of the structure. Panels b and c show the DVH parameters from the voxmin dose distribution for each patient. Panel d shows the DVH parameters from the voxmax dose distribution for each paient. (red dotted line) represent the clinical goal: D98 >38.05, V95 >98%, V107 <2%.

CTV Chestwall

The results of the robust evaluation of the chestwall (n=5) can be seen in figure 7 and table 6. The volume of the CTV chestwall decreased significantly with a mean difference of 16.18 cc. No significant difference between the planned dose and mean estimated dose of the five fractions for any of the DVH parameters was observed.

*Table 6: The results for the volume and DVH parameters (D98, V95 and V107) of the CTV Chestwall in five patients after mastectomy for pCT, dCT and difference including the associated significance *significant*

Dosimetric Parameter	pCT mean (std)	dCT mean (std)	△ mean [range]	p-value	test
Volume [cc]	421.73 (161.53)	406.27 (146.69)	16.18 [-4.50; 37.32]	0.03*	t-test
D98 [Gy]	38.67 (0.35)	38.77 (0.49)	0.04 [-0.01; 0.08]	0.44	wilcoxon signed rank test
V95 [%]	99.57 (0.46)	99.48 (0.58)	-0.09 [-0.09; 0.27]	1.0	wilcoxon signed rank test
V107 [%]	0.06 (0.12)	0.01 (0.03)	0.09 [-0.62; 1.05]	0.50	wilcoxon signed rank test

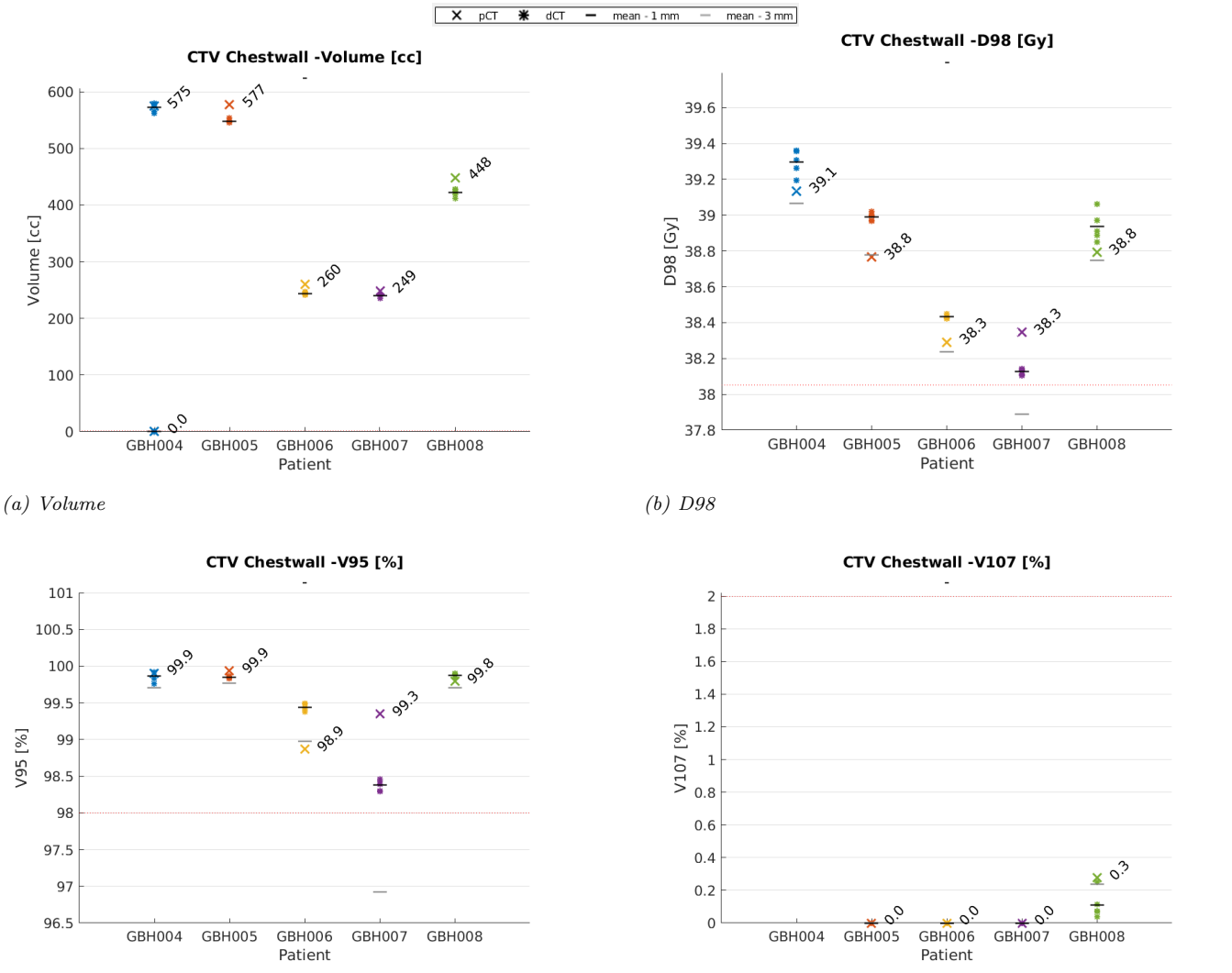

(a) Volume

(b) D98

(c) V95

(d) V107

Figure 7: Robustness evaluation of the volume, D98%, V95% and V107% for the CTV Chestwall. Panel a visualises the absolute volume of the structure. Panels b and c show the DVH parameters from the voxmin dose distribution for each patient. Panel d shows the DVH parameters from the voxmax dose distribution for each patient. (red dotted line) represent the clinical goal: D98 >38.05, V95 >98%, V107 <2%.

CTV L1 L2

The results of the robust evaluation of the CTV levels 1 and 2 (n=10) is seen in figure 8 and table 7. The volume decreased significantly, however the absolute difference was small. One patient (GBH007), the mean estimated treatment dose during the five fractions as indicated by D98 and V95 was less than the clinical goal.

*Table 7: The results for the volume and DVH parameters (D98, V95 and V107) of the CTV L1+L2 in ten patients for pCT, dCT and difference including the associated significance *significant*

Dosimetric Parameter	pCT mean (std)	dCT mean (std)	△ mean [range]	p-value	test
Volume [cc]	137.16 (31.59)	129.89 (31.61)	7.89 [-3.09; 24.79]	0.00*	t-test
D98 [Gy]	38.48 (0.17)	38.82(0.40)	-0.15 [-0.48; 1.11]	0.19	wilcoxon signed rank test
V95 [%]	99.71 (0.23)	99.47 (1.00)	-0.15 [-0.62; 4.39]	0.06	wilcoxon signed rank test
V107 [%]	0.01 (0.01)	0.02 (0.07)	-0.02 [-0.41; 0.02]	0.38	wilcoxon signed rank test

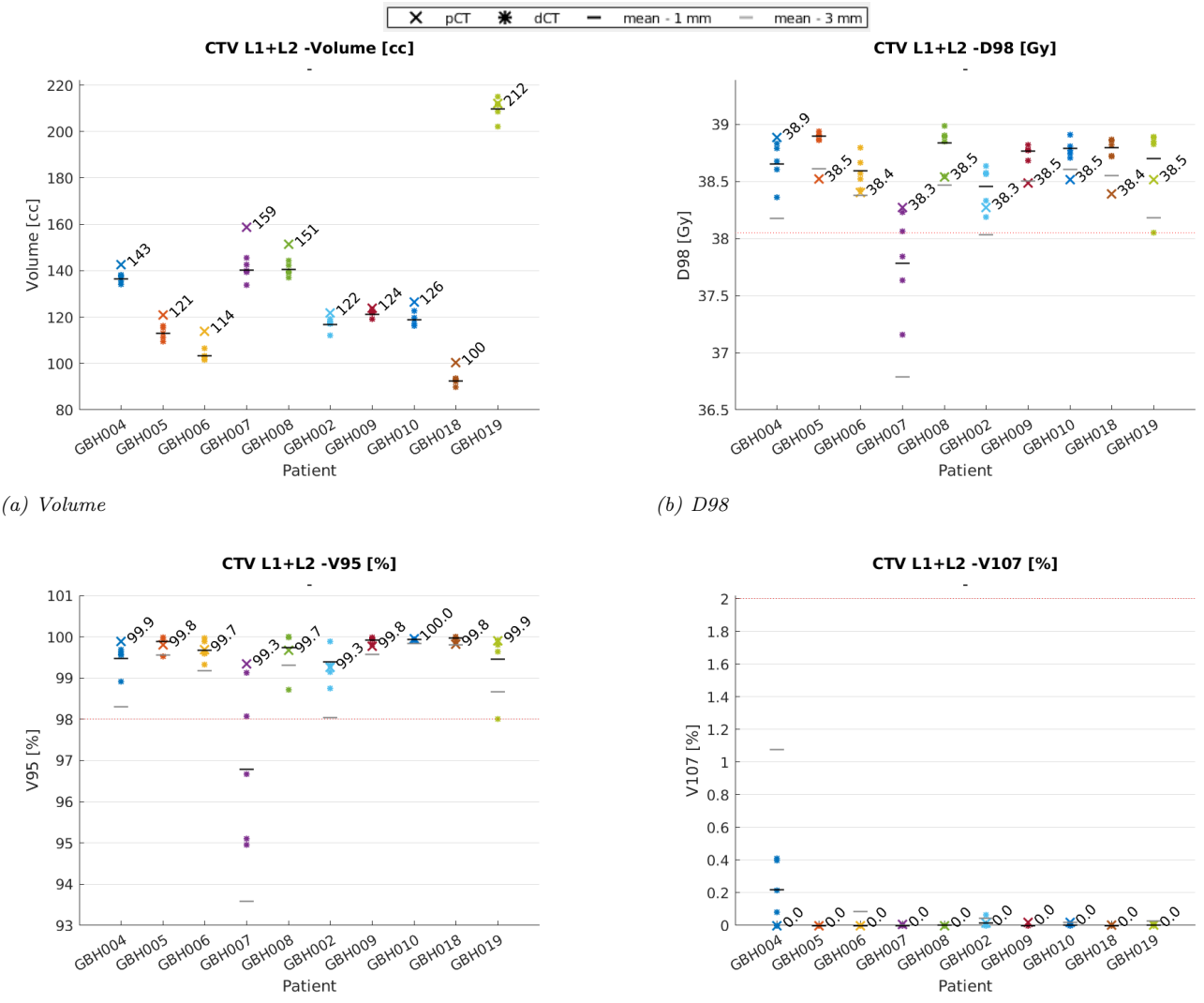

(a) Volume

(b) D98

(c) V95

(d) V107

Figure 8: Robustness evaluation of the volume, D98%, V95% and V107% for the CTV L1+L2. Panel a visualises the absolute volume of the structure. Panels b and c show the DVH parameters from the voxmin dose distribution for each patient. Panel d shows the DVH parameters from the voxmax dose distribution for each paient. (red dotted line) represent the clinical goal: D98 >38.05, V95 >98%, V107 <2%.

CTV L3 L4

The results of the robust evaluation of the CTV level 3 and 4 (n=10) can be seen in figure 9 and table 8. No difference in volume was observed between the volume of CTV level 3 and 4 on the dCT compared with the planning CT. In 11 out of 50 fractions for 10 patients the dose coverage decreased below the clinical goal. However, no significant difference between the planned dose and mean estimated dose of the five fractions for any of the DVH parameters has been observed.

*Table 8: The results for the volume and DVH parameters (D98, V95 and V107) of the CTV L3+L4 in ten patients for pCT, dCT and difference including the associated significance. *significant*

Dosimetric Parameter	**pCT mean (std)**	**dCT mean (std)**	**△ mean [range]**	**p-value**	test
Volume [cc]	29.56 (7.62)	29.46 (7.33)	0.26 [-3.01; 2.81]	0.43	t-test
D98 [Gy]	38.24 (0.20)	38.68 (0.59)	-0.11 [-0.70; 2.54]	0.38	wilcoxon signed rank test
V9 [%]	98.80 (0.63)	98.43 (2.97)	0.22 [-1.95; 13.95]	0.06	wilcoxon signed rank test
V107 [%]	0.05 (0.10)	0.04 (0.10)	0.00[-0.41; 0.33]	1.0	wilcoxon signed rank test

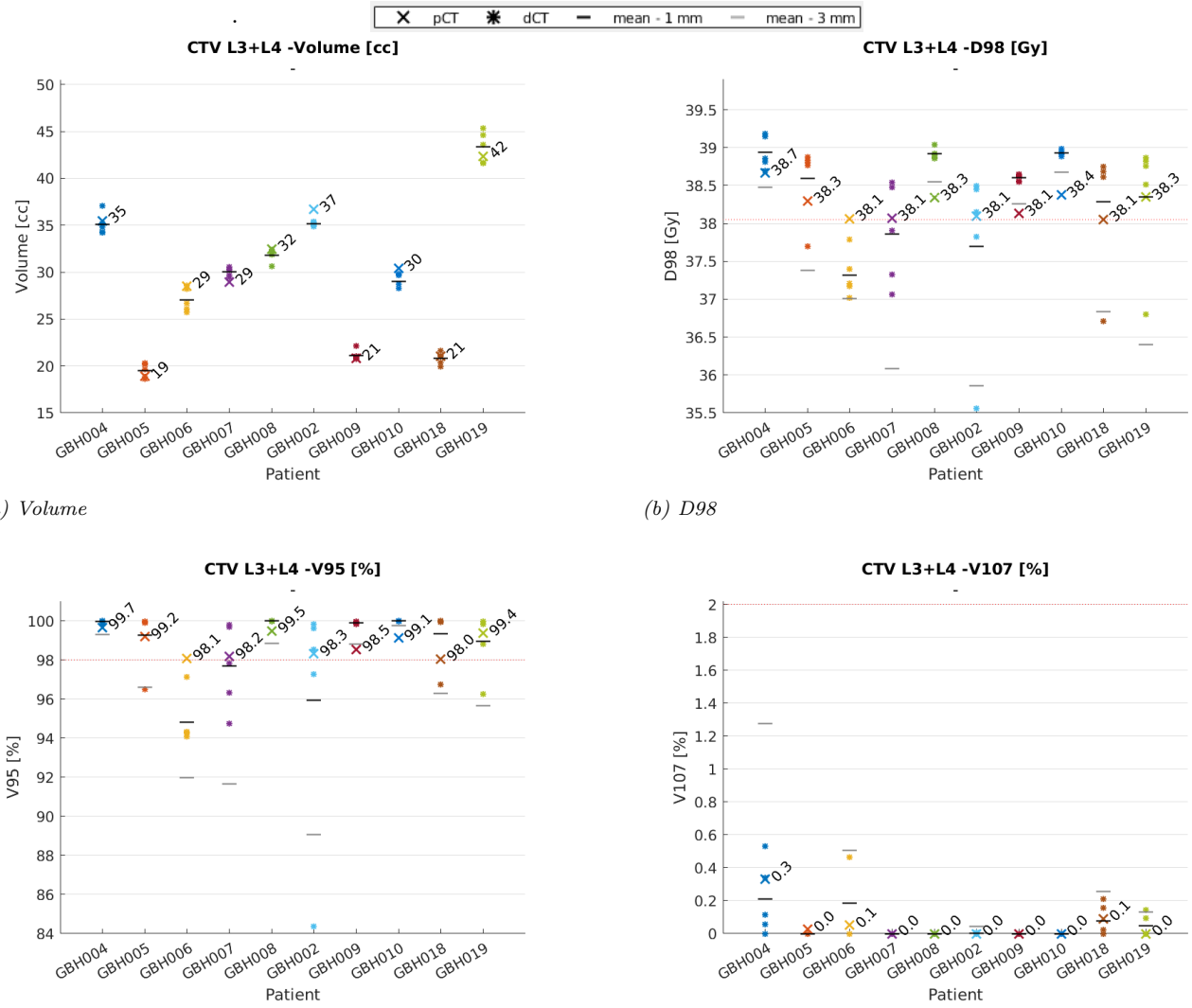

(a) Volume

(b) D98

(c) V95

(d) V107

Figure 9: Robustness evaluation of the volume, D98%, V95% and V107% for the CTV L3+L4. Panel a visualises the absolute volume of the structure. Panels b and c show the DVH parameters from the voxmin dose distribution for each patient. Panel d shows the DVH parameters from the voxmax dose distribution for each patient. (red dotted line) represent the clinical goal: D98 >38.05, V95 >98%, V107 <2%.

CTV IMC

The results of the robust evaluation of the IMC can be seen in figure 9 and table 10. No difference in volume has been observed in the volume of the CTV IMC on the dCT compared with the planning CT. In 6 out of 50 fractions for 10 patients the dose coverage decreases below the clinical goal. However, no significant difference between the planned dose and the mean estimated dose of the five fractions for any of the DVH parameters has been observed.

*Table 9: The results for the volume and DVH parameters (D98, V95 and V107) of the CTV L3+L4 in ten patients for pCT, dCT and difference including the associated significance *significant*

Dosimetric Parameter	pCT mean (std)	dCT mean (std)	△ mean [range]	p-value	test
Volume [cc]	11.10 (1.81)	10.87 (1.90)	0.24 [-1.12; 2.36]	0.19	t-test
D98 [Gy]	38.09 (0.06)	38.77 (0.35)	-0.22 [-1.00; 2.25]	0.05	wilcoxon signed rank test
V95 [%]	98.26 (0.48)	98.75 (2.20)	0.41 [-2.12; 10.13]	0.16	wilcoxon signed rank test
V107 [%]	0.00 (0.00)	0.0 (0.17)	-0.04 [-0.82; 0.00]	0.12	wilcoxon signed rank test

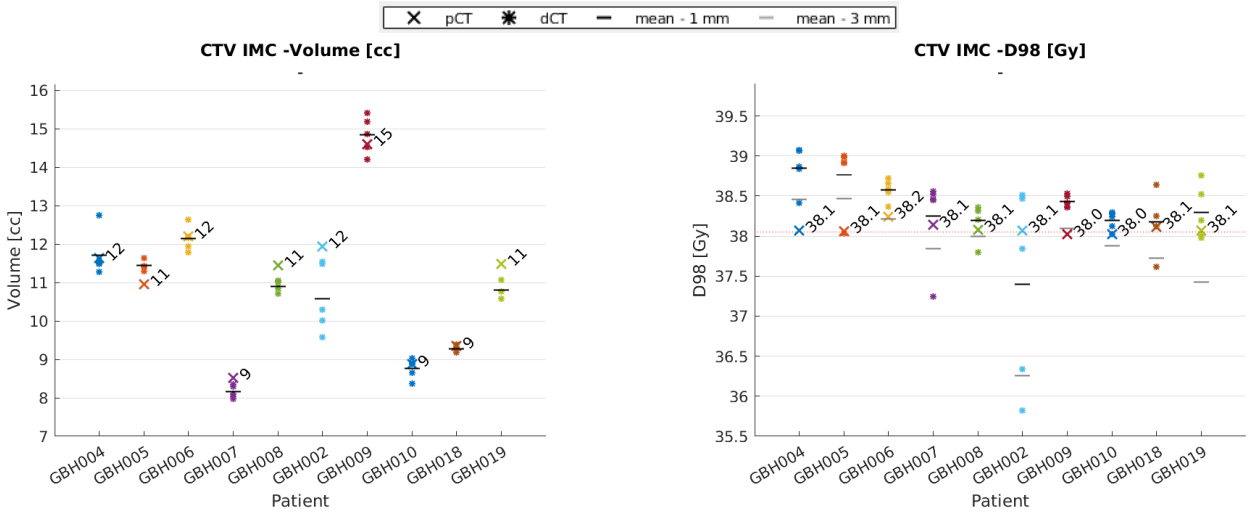

(a) Volume

(b) D98

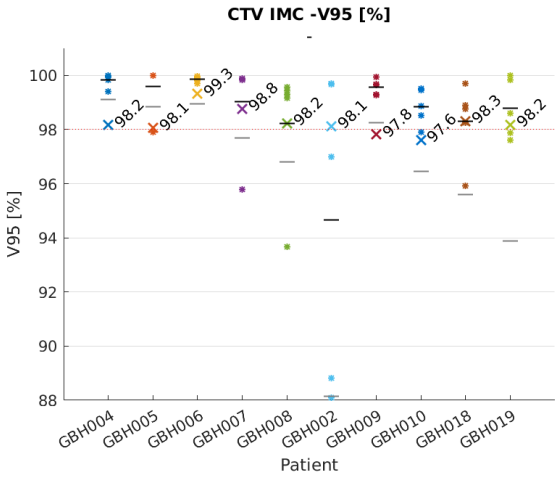

(c) V95

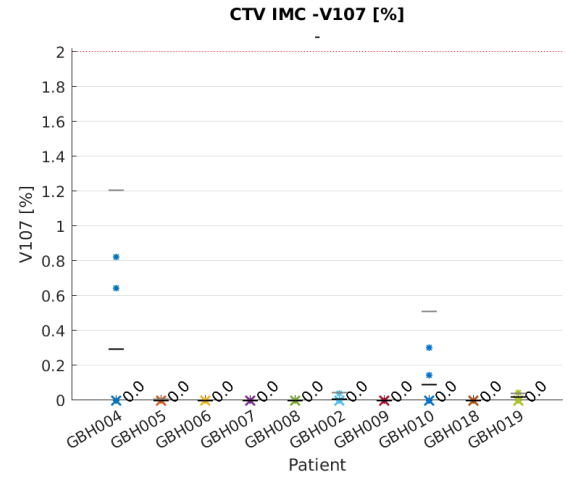

(d) V107

Figure 10: Robustness evaluation of the volume, D98%, V95% and V107% for the CTV IMC. Panel a visualises the absolute volume of the structure. Panels b and c show the DVH parameters from the voxmin dose distribution for each patient. Panel d shows the DVH parameters from the voxmax dose distribution for each paient. (red dotted line) represent the clinical goal: D98 >38.05, V95 >98%, V107 <2%.

OAR Heart

The results of the robust evaluation of the heart (n=7,10) can be seen in figure 10 and table 11. No clinically relevant difference in DVH parameters was observed.

*Table 10: The results for the volume and DVH parameters (Dmean, D2cc and V5Gy) of the Heart for pCT,dCT and difference. And the associated significance calculated by which test. N represents the number of patient included, *significant*

Dosimetric Parameter	pCT mean (std)	dCT mean (std)	△ mean [range]	p-value	test	N
Volume [cc]	649.77(87.87)	596.91 (86.62)	52.85 (19.55; 126.95)	0.01*	t-test	7
Dmean [Gy]	0.43 (0.19)	0.45(0.17)	-0.01 [0.10; 0.05]	0.47	t-test	7
D2cc [Gy]	17.02 (9.95)	17.31 (10.69)	-0.28 [-4.86; 3.03]	0.76	t-test	10
V5Gy [cc]	9.08 (7.17)	9.38 (7.66)	-0.30 [-4.26; -0.32]	0.68	t-test	10

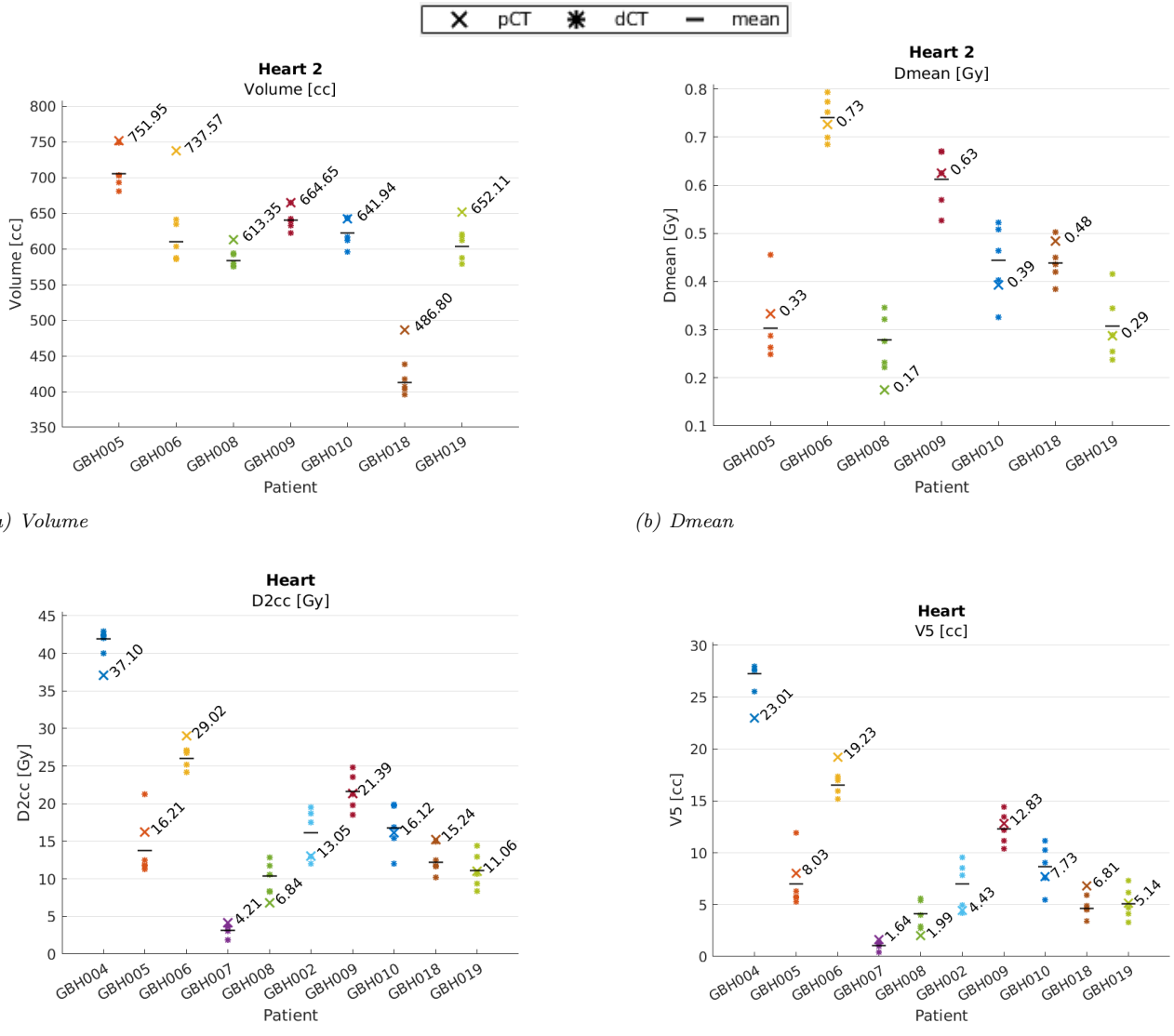

(a) Volume

(b) Dmean

(c) D2cc [Gy]

(d) V5[cc]

Figure 11: Robustness evaluation of the volume, Dmean, D2cc[Gy] and V5Gy[cc] for the Heart. Panels a shows the volume on the pCT and the estimated volume in five fractions for 7 patients Panels b shows the planned dose and estimated dose in five fractions for 7 patients of the nominal dose distribution. the DVH parameters from the voxmin dose distribution for each patient. Panels c shows the planned dose received by 2cc of the heart and estimated dose in five fractions for 10 patients. Panels d shows the volume in cc receiving 5Gy on the pCT and the estimated volume in five fractions for 10 patients

OAR Left Lung

The results of the robust evaluation of the left lung (n=10) is seen in figure 12 and table 11. Both DVH parameters showed a significant increase.

*Table 11: The results for DVH parameters (V5Gy and V20Gy) of the left lung in ten patients for pCT, dCT and difference including the associated significance *significant*

Dosimetric Parameter	pCT mean (std)	dCT mean (std)	△ mean [range]	p-value	test
V5Gy [cc]	563.28 (174.72)	620.17 (161.25)	-56.89 [-132.21;19.11]	0.00*	t-test
V20Gy [cc]	226.59 (80.38)	126.46 (38.29)	-39.04 [-66.93; -22.26]	0.00*	t-test

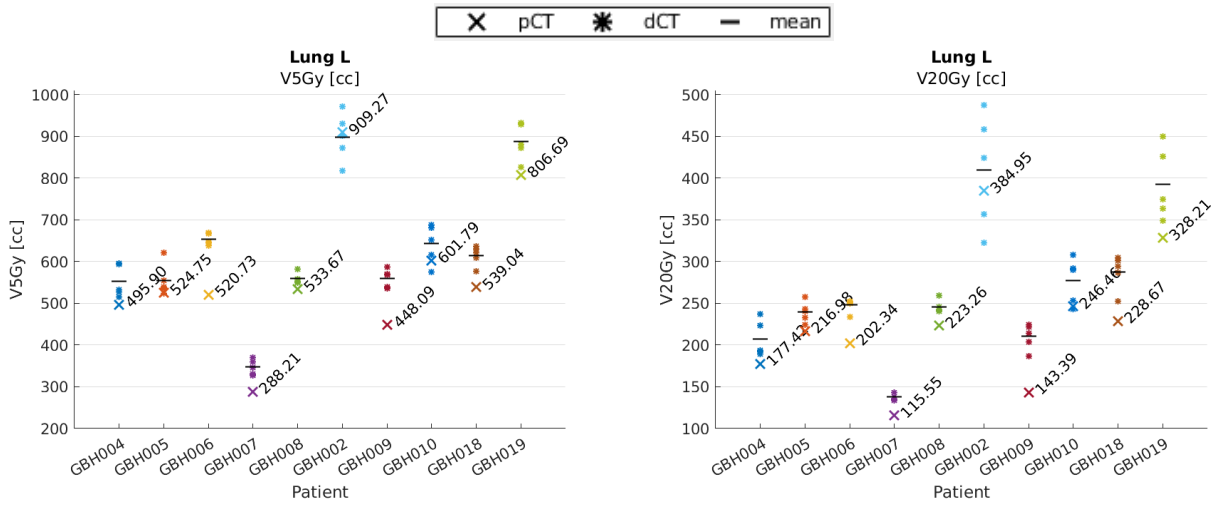

(a) V5Gy *(b) 20Gy5*

Figure 12: Robustness evaluation of the V5Gy[cc] and V20Gy[cc] for the Left lung. Panel a b showt the DVH parameters from the nominal dose distribution for each patient.

DISCUSSION

This study investigated the potential dosimetric impact of the day to day variation on proton treatment plans in patients with left-sided breast cancer with an indication for locoregional radiotherapy including IMC. We observed that the mean estimated dose distribution of five fractions was not significant different in DVH parameters for CTV Breast/Chestwall, axillary lymphnode levels 1-2, 3-4, and IMC. Only in one patient the coverage of level 1-2 fell below the clinical goal DVH parameters D98[Gy] and V95[%], and in three patients the coverage of level 3-4 fell below the clinical goal DVH parameters D98[Gy] and V95[%]. Moreover, it is interesting to note that in seven patients, the mean estimated coverage as indicated by D98 [Gy] and V95[%] increased slightly with respect to the planned dose distributions.

The cardiac dose remained low throughout the treatment period for the mean heart dose [Gy], D2cc [Gy] and V5Gy [cc]. Although the V5Gy [cc] and V20Gy[cc] of the left lung increased statistically significant, the clinical impact is limited due to the small absolute increase.

However, these results must be interpreted with caution because of various potential limitations of the methods used in this study as described below:

Accuracy of DIR and contour propagation

The accuracy of DIR and contour propagation in this study may have been limited by the quality and limited FOV of the deformed CT. The deformed CT was based on the CBCT with a limited FOV, while the pCT covers structures outside the CBCT FOV. In several patients, not all structures (in particular axillary lymph nodes level 3-4) were visualized completely (Appendix II CBCT evaluation). Thus, there is a possibility that the position of the most cranial slices of the CTV differs in clinical practice.

Moreover, the deformed CT is not entirely representative of the anatomy of the day. In this study, the pCT was deformed into the eCBCT and residual anatomy of the pCT will remain (e.g. the apex is often projected slightly more posterior on the pCT than eCBCT, or the lung volume can be transferred incorrectly). The impact of this uncertainty could not be quantified, but in the study of Hamming et al,[30] using the same methodology of deforming the pCT into the CBCT, a small difference of 0.2% (1.0%) in the average dose for CTV breast in photon VMAT was found. This suggests that the deformed CT has accurate HU values suitable for dose calculation in proton treatment plans as mentioned in other studies[31,32]

Comparing the contours derive with the semi-automatic workflow with the manually corrected contours on the eCBCT in a subset of patients, we found no systematic differences. Our study showed an MDA of 0.30 (0.2) and a DSC of 0.98 (0.1), which is similar to Hoeg et al,[33] reporting DSC of 0.80 for deformed pCT to CBCT for right-sided breast cancer patients. However, the volumes of the CTV breast/Chestwall and axillary lymhpnodes L1+L2 had a significant decrease with a small absolute difference on the dCT compared to the pCT. multiple causes could be identified: We observed a decrease in some, but not all patients. In other patients, an incorrect transfer of the most cranial and caudal slices was seen, which could induce a small volume decrease. A small difference in volume is not of clinical relevance but could introduce an apparent change in dose coverage as indicated by the increase in DVH parameters D98[Gy] and V95[%] as observed in our study. However, we observed a decrease in DVH-parameter D98[Gy], significantly for CTV L1-L2, L3-L4 and IMC, when comparing the nominal dose distribution on the pCT with the mean estimated nominal dose in five fractions (Appendix II Dose coverage nominal plan evaluation). This suggests that the small difference in volume, caused by incorrect contour deformation, is unlike to have an influence on the apparent change in dose coverage seen in this study.

Caution should be taken with generalizing the findings of this study directly to the daily clinic, as the method of registration performed for the dose evaluation in MIM differs from the clinical registration during CBCT evaluation in the clinic. The rigid registration performed in the clinic is a rigid registration with six degrees of freedom, rotational and transnational, grey level-based registration, focusing on the bony anatomy within the ROI. The rigid registration in MIM is a grey level-based registration with no focus on bony anatomy and all voxels are weighted the same. This could potentially cause a difference between the clinical and MIM registration. However, the correctness

of the applied rigid registration was checked for the alignment of the bony anatomy, and it was estimated that the impact of this uncertainty was negligible.

Parameters used for robustness evaluations

In this study, we used a robustness recipe of (5mm,3%) in accordance with clinical practice in Holland PTC. This is originally designed for free-breathing proton treatment plans. In this study, proton treatment plans were based on DIBH planning CT with the evaluation of dCT also in DIBH. There are studies indicating that the use of DIBH in proton therapy may have a positive effect on robustness because DIBH reduces intra fraction motion.[34,35] This is in line with the results of this study, which indicate that a (slightly) higher dose was delivered than was planned. This suggests that the robustness settings of 5 mm and 3% may be somewhat conservative.

The correctness of the positioning uncertainty of 1mm used in this study is difficult to determine. The dCT represents the variation in daily anatomy and patient positioning between fractions. Intra fractional variation such as DIBH reproducibility was assessed by Betgen et al[28] in patients with left-sided breast cancer treated with SGRT. The group systematic error was 0.4 +0.7, 0.4+1.4, 0.4+1.0 mm in medial-lateral (ML), anterior-posterior (AP) and cranio-caudal (CC) directions. The study of Penninkhof et al[29] shows a similar variation in the intra-fractional variation of 1.3mm in the AP direction in patients treated with SGRT (our database) The total uncertainty of 1 mm included the geometric uncertainties intra-fractional such as organ/patient movements as well as uncertainties in patient setup, e.g. uncertainties in the couch position, isocenter offset, DIBH reproducibility and heart movement as listed in Table 2.

Ultimately, a study including all fractions and the accumulated dose of the whole treatment is required to more objectively determine this. The estimated mean dose was based on five fractions instead of the given 15 fractions during the treatment course. This gives a good estimation of the systematic error, but a possible underestimation of the random error. However, it seems reasonable to assume that the application of 1 mm uncertainty combined with the DVH parameters from the voxmin dose distributions will result in a safe estimate of the actually obtained target coverage, and; the average DVH parameters from 5 fractions are a good estimator for the DVH parameters calculated from the actually delivered dose over the whole treatment.

Proton treatment plans

We were able to create proton treatment plans meeting the clinical goals for most of the patients in Erasmus-iCycle with the created wish-list. Erasmus-iCycle was not able to achieve the clinical goal (D98>95%PD) for CTV IMC in two patients with glandular breast tissue and for this reason, a non critical under dosage of D98>94% was accepted. Of note, for photon plans D98% >90% is often used in daily clinical practice in line with a national consensus.[36] During optimization and evaluation, the CTV dose on the voxel-wise minimum and maximum dose had to achieve the PTV-based clinical goals mentioned in 1 in compliance with HollandPTC's clinical protocol. The study of korevaar et al[26] showed that the voxel-wise minimum and maximum dose criteria for CTV D98 and D2 show very strong correlations to PTV D98% [Gy] and D2% [Gy] and, on average, required adjustments of 0.9% and +2.3%, respectively. This implies that the straightforward conversion of PTV constraints to CTV constraints on voxel-wise scenarios is overly cautious and that the voxel-wise minimum and maximum constraints can be lowered. With this in mind, it could be suggested that the also the clinical goals for CTV IMC in patient GBH009 and GBH0010 achieve enough coverage.

These treatment plans were evaluated on 19 scenarios, including the set-up error of 5 mm in the six cardinal axis and range uncertainties of -3%, 0% and +3% (3x6=18 scenarios) plus nominal plan with 0% range uncertainties. In clinical practice at Holland PTC the robustness evaluation exists of 29 scenarios. These additional scenarios include eight scenarios with a 5 mm set-up uncertainties along the diagonal axis and range uncertainties of -3% and +3% (2x14=28 scenarios) plus the nominal scenario. From these 29 scenarios, the voxmin Dose and the voxmax dose are used for evaluation. Since our plans were evaluated on less scenarios, the plans may be less robust.

In this study, the planned treatment isocenter differs from the treatment isocenter chosen in clinical practice at Holland PTC. However, the proton treatment plans were checked by an experienced breast radiation oncologist and

were considered clinically accepted plans. It is therefore assumed that within the scope of this study this effect is negligible. However, it should be taken into account when implementing this in clinical practice.

Study size

Another limitation is the small number of patients. The generalization of the results could be limited because of the small sample size. If data from more patients had been included, a larger variation in patient anatomy would have been included in the study, increasing the generalization of results. However, we assume that our patient population is reasonably representative of the left-sided breast cancer population, as we purposely selected five patients with chestwall and five patients with breast glandular tissue.

Reproducibility of DIBH

In this study, patients were positioned with an optical surface tracking system and verified by CBCT. SGRT has the ability of beam gating, when the breathing signal is within a specified gating window and the distance between the patient's real-time surface and the reference surface is within the tolerances, the SGRT DIBH clinical procedure permits radiation delivery. The accuracy of treatment delivery may be impacted by the use of these beam-on thresholds. This raises the question of whether the plans generated in this study are robust enough to these uncertainties such as wider variation in DIBH. The average chest motion for respiratory motion is 1.8-2.0, so we expect to be well within the possible intra fractional errors at 3 mm when irradiating a patient in DIBH without beam gating. It was observed that the deviant values were more variant in the evaluation with robustness setting (3mm,3) (Appendix II, III Robustness evaluation 3 mm analysis). For CTV L1 and L2, this has no clinical consequences because adequate coverage is still achieved. However, with a mean difference of 3.00% the V95 [%] drops to a mean value of 95,79% for all 10 patients. This could imply that CTV L3+L4 does not account for a geometric variation of 3 mm.

Presence of metal objects in one patient

Patient six had a metal plate on her collarbone, making her not a right fit for proton therapy. Both during the calculation during pCT and dCT there was no overwrite given in terms of stopping power prediction to this structure. This structure was in the levels of CTV L3-L4 and this causes a drop in dose coverage in the V95[%] of patient GBH006.

Future research

This study focuses on the inter fractional variation between fractions during the course of proton treatment plans with the dCT, and intra fractional variation with the robustness evaluation within a fraction. The shifts in the isocenter of 1 mm are calculated on the dose distribution of fraction or 3 beams together. It would be interesting to see what effect the difference in DIBH has on the individual beams. Further research could identify the optimal robustness setting for proton treatment plans in patients with left-sided breast cancer treated in DIBH. In this study, only robustness settings of (5mm, 3%) has been investigated, and showed that target coverage was easily achieved in all CTVs. Therefore, we suggest further research could focus on evaluating new robustness setting for example decreasing the geometric error to a robustness setting to (3mm, 3%).

CONCLUSION

Proton treatment plans, created in Erasmus-iCycle, achieve coverage above the clinical goals in the mean estimated delivered dose of five fractions in patient with left-sided breast cancer patients with indication for irradiation of the breast/chestwall, axillary lymph nodes and IMC treated with image guided radiotherapy and surface guidance for DIBH.

REFERENCES

1. NKI borstkanker incidentie Kernel Description https://iknl.nl/nkr/uitleg-NKR-cijfers. Accessed: 2023-01-06.
2. Group EBCTC, others . Effect of radiotherapy after breast-conserving surgery on 10-year recurrence and 15-year breast cancer death: meta-analysis of individual patient data for 10 801 women in 17 randomised trials *The Lancet.* 2011;378(9804):1707–1716.
3. Darby SC, McGale P, Taylor CW, Peto R. Long-term mortality from heart disease and lung cancer after radiotherapy for early breast cancer: prospective cohort study of about 300 000 women in US SEER cancer registries *The lancet oncology.* 2005;6(8):557–565.
4. Correa CR, Litt HI, Hwang WT, Ferrari VA, Solin LJ, Harris EE. Coronary artery findings after left-sided compared with right-sided radiation treatment for early-stage breast cancer *Journal of clinical oncology.* 2007;25(21):3031–3037.
5. Darby SC, Ewertz M, McGale P, *et al.* Risk of ischemic heart disease in women after radiotherapy for breast cancer *New England Journal of Medicine.* 2013;368(11):987–998.
6. Bogaard VA, Ta BD, Schaaf A, *et al.* Validation and modification of a prediction model for acute cardiac events in patients with breast cancer treated with radiotherapy based on three-dimensional dose distributions to cardiac substructures *Journal of Clinical Oncology.* 2017;35(11):1171.
7. Zhu Q, Kirova YM, Cao L, Arsene-Henry A, Chen J. Cardiotoxicity associated with radiotherapy in breast cancer: a question-based review with current literatures *Cancer treatment reviews.* 2018;68:9–15.
8. Latty D, Stuart KE, Wang W, Ahern V. Review of deep inspiration breath-hold techniques for the treatment of breast cancer *Journal of medical radiation sciences.* 2015;62(1):74–81.
9. Langendijk JA, Lambin P, De Ruysscher D, Widder J, Bos M, Verheij M. Selection of patients for radiotherapy with protons aiming at reduction of side effects: the model-based approach *Radiotherapy and Oncology.* 2013;107(3):267–273.
10. Bujold A, Craig T, Jaffray D, Dawson LA. Image-guided radiotherapy: has it influenced patient outcomes? in *Seminars in radiation oncology*;22:50–61Elsevier 2012.
11. Van Herk M. Errors and margins in radiotherapy in *Seminars in radiation oncology*;14:52–64Elsevier 2004.
12. Yan D, Vicini F, Wong J, Martinez A. Adaptive radiation therapy *Physics in Medicine & Biology.* 1997;42(1):123.
13. Schulze R, Heil U, Groβ D, *et al.* Artefacts in CBCT: a review *Dentomaxillofacial Radiology.* 2011;40(5):265–273.
14. Zhen X, Gu X, Yan H, Zhou L, Jia X, Jiang SB. CT to cone-beam CT deformable registration with simultaneous intensity correction *Physics in Medicine & Biology.* 2012;57(21):6807.
15. Veiga C, McClelland J, Moinuddin S, *et al.* Toward adaptive radiotherapy for head and neck patients: feasibility study on using CT-to-CBCT deformable registration for "dose of the day" calculations *Medical physics.* 2014;41(3):031703.
16. Veiga C, Janssens G, Teng CL, *et al.* First clinical investigation of cone beam computed tomography and deformable registration for adaptive proton therapy for lung cancer *International Journal of Radiation Oncology* Biology* Physics.* 2016;95(1):549–559.
17. Offersen BV, Boersma LJ, Kirkove C, *et al.* ESTRO consensus guideline on target volume delineation for elective radiation therapy of early stage breast cancer *Radiotherapy and oncology.* 2015;114(1):3–10.

18. Feng M, Moran JM, Koelling T, *et al.* Development and validation of a heart atlas to study cardiac exposure to radiation following treatment for breast cancer *International Journal of Radiation Oncology* Biology* Physics.* 2011;79(1):10–18.

19. Liu Y, Jin R, Chen M, *et al.* Contour propagation using non-uniform cubic B-splines for lung tumor delineation in 4D-CT *International journal of computer assisted radiology and surgery.* 2016;11(12):2139–2151.

20. Peroni M, Spadea M, Riboldi M, *et al.* Validation of automatic contour propagation for 4D treatment planning using multiple metrics *Technology in cancer research & treatment.* 2013;12(6):501–510.

21. Dice LR. Measures of the amount of ecologic association between species *Ecology.* 1945;26(3):297–302.

22. Chalana V, Kim Y. A methodology for evaluation of boundary detection algorithms on medical images *IEEE Transactions on medical imaging.* 1997;16(5):642–652.

23. Breedveld S, Storchi PR, Voet PW, Heijmen BJ. iCycle: Integrated, multicriterial beam angle, and profile optimization for generation of coplanar and noncoplanar IMRT plans *Medical physics.* 2012;39(2):951–963.

24. Lomax A. Intensity modulated proton therapy and its sensitivity to treatment uncertainties 2: the potential effects of inter-fraction and inter-field motions *Physics in Medicine & Biology.* 2008;53(4):1043.

25. Ödén J, Eriksson K, Toma-Dasu I. Incorporation of relative biological effectiveness uncertainties into proton plan robustness evaluation *Acta oncologica.* 2017;56(6):769–778.

26. Korevaar EW, Habraken SJ, Scandurra D, *et al.* Practical robustness evaluation in radiotherapy–A photon and proton-proof alternative to PTV-based plan evaluation *Radiotherapy and Oncology.* 2019;141:267–274.

27. Rojo-Santiago J, Habraken SJ, Lathouwers D, Romero AM, Perkó Z, Hoogeman MS. Accurate assessment of a Dutch practical robustness evaluation protocol in clinical PT with pencil beam scanning for neurological tumors *Radiotherapy and Oncology.* 2021;163:121–127.

28. Betgen A, Alderliesten T, Sonke JJ, Vliet-Vroegindeweij C, Bartelink H, Remeijer P. Assessment of set-up variability during deep inspiration breath hold radiotherapy for breast cancer patients by 3D-surface imaging *Radiotherapy and Oncology.* 2013;106(2):225–230.

29. Penninkhof J, Fremeijer K, Harten K, *et al.* Evaluation of image-guided and surface-guided radiotherapy for breast cancer patients treated in deep inspiration breath-hold: A single institution experience *Technical innovations & patient support in radiation oncology.* 2022;21:51–57.

30. Hamming VC, Andersson S, Maduro JH, Langendijk JA, Both S, Sijtsema NM. Daily dose evaluation based on corrected CBCTs for breast cancer patients: accuracy of dose and complication risk assessment *Radiation Oncology.* 2022;17(1):1–11.

31. Thummerer A, Zaffino P, Meijers A, *et al.* Comparison of CBCT based synthetic CT methods suitable for proton dose calculations in adaptive proton therapy *Physics in Medicine & Biology.* 2020;65(9):095002.

32. Veiga C, Janssens G, Baudier T, *et al.* A comprehensive evaluation of the accuracy of CBCT and deformable registration based dose calculation in lung proton therapy *Biomedical Physics & Engineering Express.* 2017;3(1):015003.

33. Høeg A. ROBUSTNESS ANALYSIS OF RADIATION TREATMENT PLANS FOR BREAST CANCER, A COMPARATIVE STUDY BETWEEN PROTONS AND PHOTONS Master's thesisNTNU 2019.

34. Mast ME, Vredeveld EJ, Credoe HM, *et al.* Whole breast proton irradiation for maximal reduction of heart dose in breast cancer patients *Breast cancer research and treatment.* 2014;148(1):33–39.

35. Ranger A, Dunlop A, Hutchinson K, *et al.* A dosimetric comparison of breast radiotherapy techniques to treat locoregional lymph nodes including the internal mammary chain *Clinical Oncology.* 2018;30(6):346–353.

36. Hurkmans C, Duisters C, Peters-Verhoeven M, *et al.* Harmonization of breast cancer radiotherapy treatment planning in the Netherlands *Technical innovations & patient support in radiation oncology.* 2021;19:26–32.

APPENDIX I: SUPPLEMENTARY MATERIALS

DIR specifications

The MIM Software (MIM Sofware Inc., Cleveland, OH) deformable image registration workflows were used to generate a deformed planning CT. This was done with three seperate worfklows. In this table the specification for the used registration algorithms are mentioned. The free-from deformation uses a feature similarity scoring metric. It aims to maximize the correspondence of high-dimensional featur edescriptors computed by evaluating each image voxel in the context of its neighboring voxels. The smoothness factor provides the ability to control the smoothness of the deformation.(smal numbers means less smoothing). Normalization can be used for cases where intensities between images are inconsistent (e.g. CT-CBCT). Normalization uses a bi-linear model to normalize the intensities of one iamge to match those of the other. Dynamic Regularization is used to provide less smoothing in areas with sufficient information to help drive the deformation and more smoothing in areas with less information to prevent unrealistic deformations from occurring.

Table 12: Specifications of the registrations used in the semi-automatic workflow

Workflow	Image regsitration	Specifications	Optimization settings
Step 1	Rigid Transformation	Six degrees of freedom, rotational and translational	-
Step 2	Deformable image registration	Free-form, unlimited degrees of freedom	Smoothness factor 0.5 Normalization
Step 3	Deformable image registration	Free-form, unlimited degrees of freedom	Smoothness factor 1.5 Dynamic regularization

Imperfections eCBCT

The enhance CBCT is the result of the first two sub-workflows. Figure 13 shows that the eCBCT is not suitable for dose calculation for several reasons. First, an part of the pCT is shown within the red structure. This is because the chest wall tissue shrinks, making it smaller than the chest wall contour of the pCT. This results in incorrect daily anatomy, as there should be no additional tissue behind the patient contour on the part of the CBCT on the eCBCt. Second, shading artefacts are still visible, which may affect the dose calculation. Third, visual inspection shows that the HU intensities on the eCBCT have been improved compared with the original CBCT. However, Figure 15 shows that the distribution histogram of all HU intensities within the structure Breast on the eCBCT (Fig. 15b) does not match the histogram on the on the pCT (Fig. 15a). The third workflow eliminates these shortcomings, as you can see in Figure 14 and in Figure (Fig. **??**) by comparing the histogram of the dCT with the histogram of the pCT.

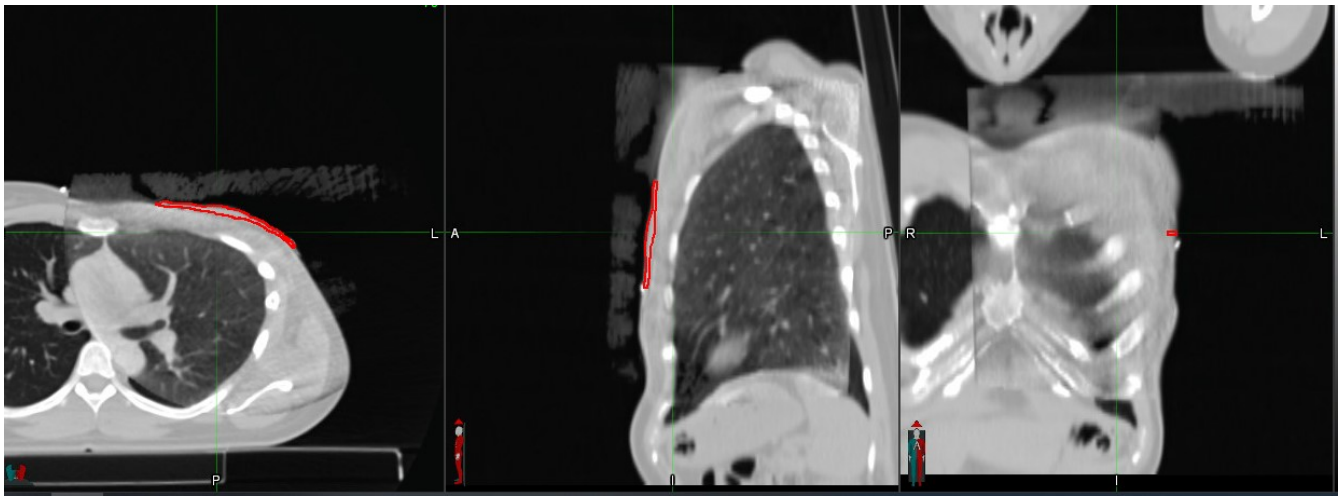

Figure 13: Shortcomings of eCBCT to perform dose calculations. 1) Inside the red structure voxels of the patient on the pCT is visible. 2) Remaining shading artefacts 3) HU intensties not suitable for dose calculation

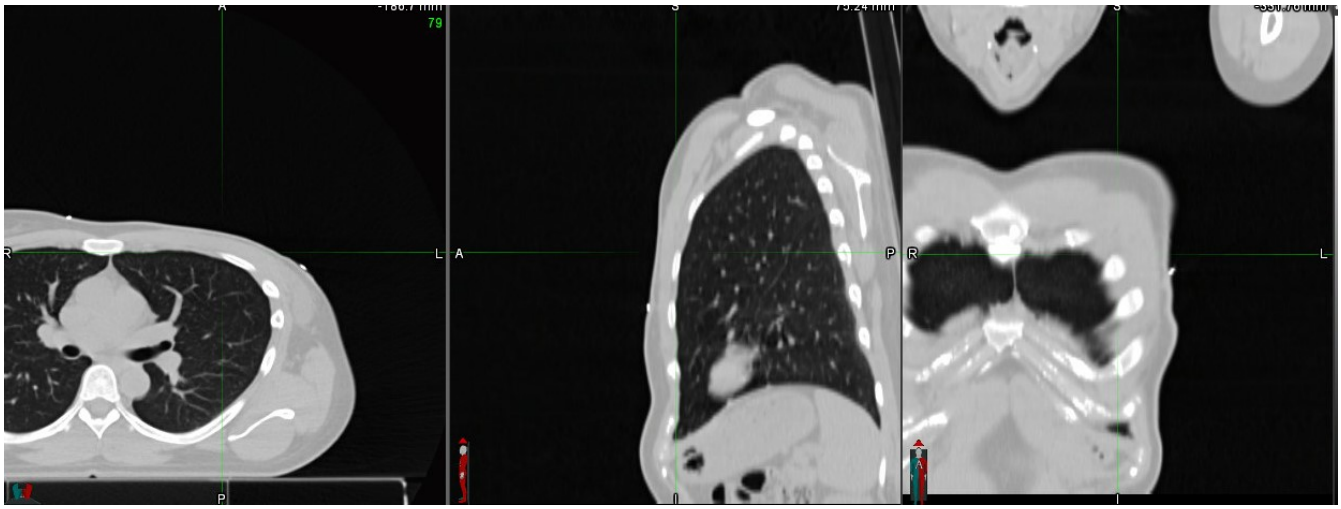

Figure 14: dCT without shortcomings of eCBCT. 1) no remaining pCT part in CBCT FOV. 2) no remaining shading artefacts. 3) HU intenstities suitable for dose calcuation

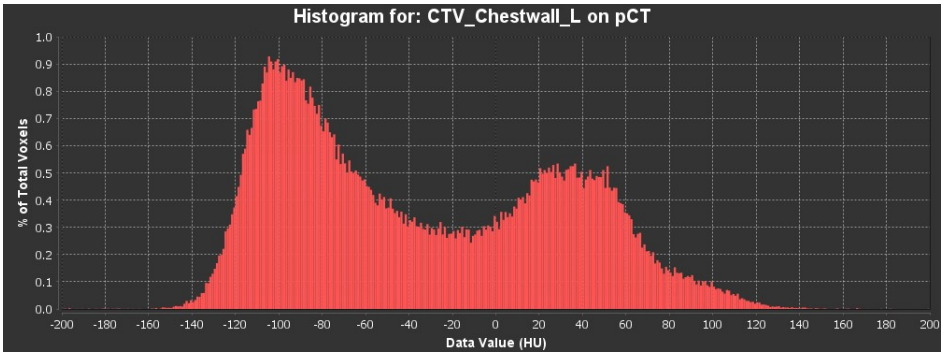

(a) Histogram of HU intenstities of all voxel of the structure CTV Chestwall L on the pCT

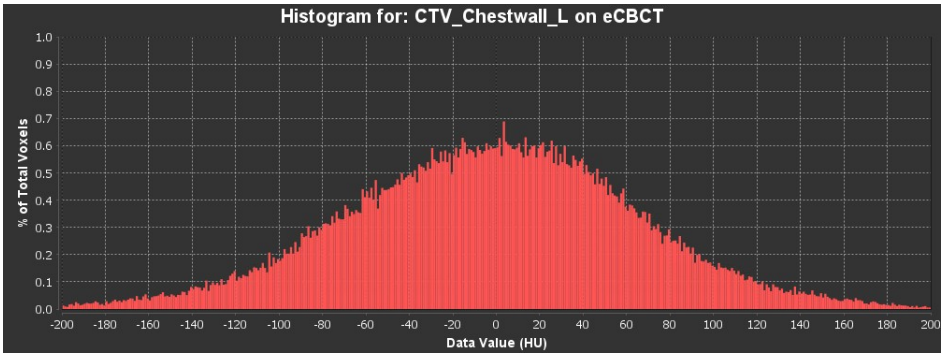

(b) Histogram of HU intenstities of all voxel of the structure CTV Chestwall L on the eCBCT

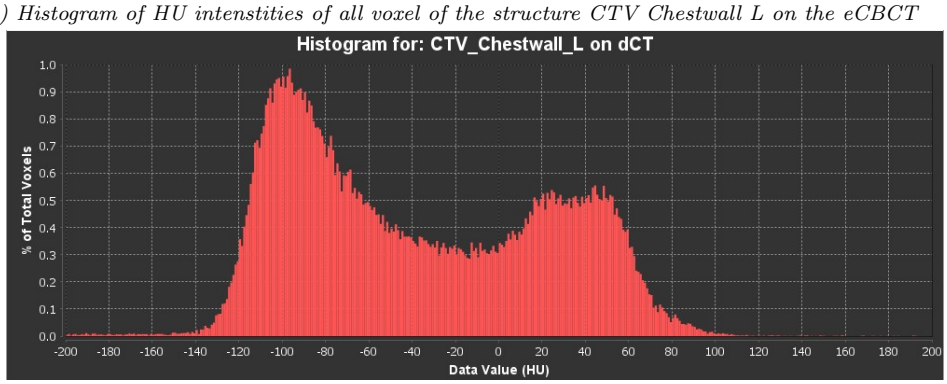

(c) Histogram of HU intenstities of all voxel of the structure CTV Chestwall L on the eCBCT

Figure 15: Difference in Histograms for CTV Chestwall

I-cycle Wishlist

Erasmus-iCycle wishlist for intensity modulated proton plans (IMPT) for whole breast/Chestwall including axillary lymphnodes and IMC. When a rule is given priority constrain this rule is never violated, while the rules given with a number for priority (objectives) are optimized one at a time The priority numbers indicate the order in which the objectives are being optimized: lower numbers have higher priorities. The following structures are defined in the wishlist:

- The structures CTV Total shell 1mm refers to a shell of 1 mm width around the CTV at distances of 0 mm.
- The structures CTV Total ring 0-5mm, CTV Total ring 5-10mm and CTV Total ring 10-15mm refer to rings of 5mm width around the CTV at distances of 0, 5 and 10 mm from the structure, respectively.
- The structures CTV IMC ring 0-5mm and CTV IMC ring 5-10 mm and CTV Total ring 10-15mm refer to rings of 5mm width around the CTV IMC at distances of 0 and 5 mm from the structure, respectively.

The prescribed dose is denoted by 40.05 [Gy], in 15 fractions. Plans were robustly optimized using 19 different scenarios for 5 mm setup uncertainty and 3% range uncertainty. In column Type linear or Mean is chosen. Linear means that the rule applies on one voxel, the voxel with the most dose or least dose. Mean reflects on the mean dosis of the specified structure. In the column Robust it can be chosen wheter the rule should applied only in the nominal plan or at all the 19 scenarios used in the robustness evaluation.

Table 13: Wishlist IMPT Breast/Chestwall including Axillary lymph nodes level 1-4 + IMC B is breast, C is chestwall

Priority B	C	Structure	Min/Max	Type	Goal	Robust
Constraint	Constraint	CTV_Breast_L-05	Maximize (minimum)	Linear	A*0.99	Yes
Constraint	Constraint	CTV_L1+L4	Maximize (minimum)	Linear	A*0.99	Yes
Constraint	Constraint	CTV_IMC	Maximize (minimum)	Linear	A*0.99	Yes
Constraint	Constraint	CTV_Total_shell_1mm	Maximize (minimum)	Linear	A*0.97	Yes
1	1	CTV_Breast_L-05	Minimize (maximum)	Linear	A*1.06	Yes
1	1	CTV_L1+L4	Minimize (maximum)	Linear	A*1.06	Yes
1	1	CTV_IMC	Minimize (maximum)	Linear	A*1.06	Yes
2	2	CTV_Total_ring_0-5mm	Minimize (maximum)	Linear	A*1.03	No
2	2	CTV_IMC_ring_0-5mm	Minimize (maximum)	Linear	A*1.03	No
2	2	CTV_Total_ring_5-10mm	Minimize (maximum)	Linear	A*0.95	No
2	2	CTV_IMC_ring_5-10mm	Minimize (maximum)	Linear	A*0.95	No
2	2	CTV_Total_ring_10-15mm	Minimize (maximum)	Linear	A*0.93	No
2	-	Skin-03	Minimize (maximum)	Linear	A*0.99	No
3	3	Heart	Minimize (maximum)	Linear	10	Yes
3	3	Heart	Minimize (maximum)	Mean	2.5	No
4	4	Lung_L	Minimize (maximum)	Mean	1	No
5	5	Breast_R	Minimize (maximum)	Mean	0.5	No
6	6	Lung_R	Minimize (maximum)	Mean	1	No
7	7	CTV_ring_0-5mm	Minimize (maximum)	Mean	1	No
7	7	CTV_ring_5-10mm	Minimize (maximum)	Mean	1	No
7	7	CTV_ring_10-15mm	Minimize (maximum)	Mean	1	No
8	8	Patient	Minimize (maximum)	Linear	1	No
9	9	MU	Minimize (maximum)	Linear	1	No

Table 14: Optimization settings used in treatment optimization proton plans

Optimization settings	
Beam angles [degree]	10, 50, 340
Setup robustness [mm]	5
Range robustness [%]	3
Number of iterations	8
Bixelgrid [mm]	2
Dose grid [mm]	3
Spot margin [mm]	5

APPENDIX II: SUPPLEMENTARY TABLES

Robustness evaluation 3 mm analysis

*Table 15: Statistics for DVH for all CTVs from all patients for pCT, dCT and difference with robustness settings 3mm. Plus the significance calculated whit which test. *significant*

CTV	Parameter	pCT mean (std)	dCT mean (std)	diff mean [range]	p-value	test
Breast	D98	39.11(0.14)	38.67 (0.21)	-0.02 [-0.12;0.21]	0.62	wilcoxon signe rank test
	V95	99.92 (0.04)	99.75 (0.35)	0.18 [-0.07; 0.79]	0.44	wilcoxon signe rank test
	V107	0.49 (0.85)	0.15 (0.19)	0.34 [-0.00; 1.31]	0.12	wilcoxon signe rank test
Chestwall	D98	38.67 (0.35)	38.54 (0.47)	0.12 [-0.01; 0.46]	0.12	wilcoxon signe rank test
	V95	99.57 (0.46)	99.02 (1.21)	0.55 [-0.11; 2.42]	0.19	wilcoxon signe rank test
	V107	0.06 (0.12)	0.05 (0.11)	0.01 [-0.00; 0.04]	0.50	wilcoxon signe rank test
L1 L2	D98	38.48 (0.17)	38.23 (0.17)	0.25 [0.16;1.48]	0.28	wilcoxon signe rank test
	V95	99.71(0.23)	98.58 (1.86)	1.13 [0.02; 5.76]	0.00*	wilcoxon signe rank test
	V107	0.01 (0.01)	0.13 (0.34)	-0.12 [1.08; 0.02]	0.25	wilcoxon signe rank test
L3 L4	D98	38.24 (0.20)	37.35 (1.08)	0.89 [-0.30; 2.24]	0.05	wilcoxon signe rank test
	V95	98.80 (0.63)	95.79 (3.72)	3.00 [-0.63;9.25]	0.01*	wilcoxon signe rank test
	V107	0.05 (0.10)	0.22 (0.41)	-0.17 [-0.95;0.03]	0.06	wilcoxon signe rank test
IMC	D98	38.09 (0.06)	37.84 (0.64)	0.25 [-0.41;1.81]	0.32	wilcoxon signe rank test
	V95	98.26 (0.48)	96.37 (3.34)	1.89 [-0.94; 9.98]	0.06	wilcoxon signe rank test
	V107	0.18 (0.39)	0.18 (0.39)	-0.18 [-1.21; 0.00]	0.06	wilcoxon signe rank test

CBCT evaluation

Table 16: Visually inspection of the CBCT if the structure is captured entirely.

	Patient Name	Chestwall/mamma	L1+L2	L3+L4	IMC	Heart	Lung_L
Chestwall	GBH004	ja	ja	nee	ja	nee	nee
Chestwall	GBH005	ja	ja	ja	ja	ja	nee
Chestwall	GBH006	ja	ja	ja	ja	ja	nee
Chestwall	GBH007	ja	ja	ja	ja	nee	nee
Chestwall	GBH008	ja	nee	nee	nee	ja	nee
Breast	GBH002	ja	nee	nee	ja	nee	nee
Breast	GBH009	ja	ja	nee	ja	ja	nee
Breast	GBH010	ja	nee	nee	nee	ja	nee
Breast	GBH018	ja	ja	ja	ja	ja	nee
Breast	GBH019	ja	ja	ja	ja	ja	nee

Dose coverage nominal plan evaluation

*Table 17: Statistics for DVH D98 for all CTVs from all patients for pCT, dCT and difference. Plus the significance calculated whit which test. *significant*

CTV	Parameter	pCT mean (std)	dCT mean (std)	diff mean [range]	p-value	test
Breast	D98	39.21 (0.15)	39.07 (0.22)	0.14 [0.06; 0.29]	0.06	wilcoxon signed rank test
Chestwall	D98	39.27 (0.37)	38.95 (0.50)	0.32 [0.14; 0.60]	0.06	wilcoxon signed rank test
L1 L2	D98	39.22 (0.21)	38.97 (0.32)	0.24 [0.07; 0.66]	0.00	wilcoxon signed rank test
L3 L4	D98	39.16 (0.23)	38.86 (0.44)	0.30 [0.06; 1.12]	0.00	wilcoxon signed rank test
IMC	D98	39.25 (0.18)	38.90 (0.28)	0.35 [0.14; 0.70]	0.00	wilcoxon signed rank test

Shapiro wilk tests

Table 18: Shapiro wilk test MIM validation

Structure	Parameter	Shapiro-Wilk test	W	p	N	a=0,01	a=0,05	Test
CTV Chestwal /Breast	Volume	<var>	0.753	0.005	15	not normal	not normal	wilcoxon signed rank test
	D98	<var>	0.671	0.003	15	not normal	not normal	wilcoxon signed rank test
	V95	<var>	0.879	0.021	15	normal	not normal	t-test
CTV L1+ L2	Volume	<var>	0.707	0.005	11	not normal	not normal	wilcoxon signed rank test
	D98	<var>	0.817	0.014	11	normal	not normal	t-test
	V95	<var>	0.537	0.001	15	not normal	not normal	wilcoxon signed rank test
Heart	Volume	<var>	0.094	0.000	11	not normal	not normal	wilcoxon signed rank test
	Dmean	<var>	0.305	0.001	11	not normal	not normal	wilcoxon signed rank test
	D2cc	<var>	0.305	0.001	11	not normal	not normal	wilcoxon signed rank test

Table 19: Shapiro wilk test output for DVH paramters for each CTV

Structure	Parameter	Shapiro-Wilk test	W	p	N	a=0,01	a=0,05	test
CTV Breast	Volume	<var>	0.90	0.02	25	normal	not normal	t-test
	D98	<var>	0.67	0.00	25	not normal	not normal	wilcoxon signed rank test
	V95	<var>	0.37	0.00	25	not normal	not normal	wilcoxon signed rank test
	V107	<var>	0.64	0.00	25	not normal	not normal	wilcoxon signed rank test
CTV Chestwall	Volume	<var>	0.97	0.15	25	normal	normal	t-test
	D98	<var>	0.79	0.00	25	not normal	not normal	wilcoxon signed rank test
	V95	<var>	0.86	0.01	25	not normal	not normal	wilcoxon signed rank test
	V107	<var>	0.49	0.00	25	not normal	not normal	wilcoxon signed rank test
CTV L1+ L2	Volume	<var>	0.96	0.05	50	normal	normal	t-test
	D98	<var>	0.79	0.00	50	not normal	not normal	wilcoxon signed rank test
	V95	<var>	0.60	0.00	50	not normal	not normal	wilcoxon signed rank test
	V107	<var>	0.37	0.00	50	not normal	not normal	wilcoxon signed rank test
CTV L3+L4	Volume	<var>	0.98	0.14	50	normal	normal	t-test
	D98	<var>	0.74	0.00	50	not normal	not normal	wilcoxon signed rank test
	V95	<var>	0.65	0.00	50	not normal	not normal	wilcoxon signed rank test
	V107	<var>	0.72	0.00	50	not normal	not normal	wilcoxon signed rank test
CTV IMC	Volume	<var>	0.92	0.01	50	normal	not normal	t-test
	D98	<var>	0.79	0.00	50	not normal	not normal	wilcoxon signed rank test
	V95	<var>	0.59	0.00	50	not normal	not normal	wilcoxon signed rank test
	V107	<var>	0.30	0.00	50	not normal	not normal	wilcoxon signed rank test

Table 20: Shapiro wilk test output for DVH paramters for each OAR.

Structure	Parameter	Shapiro-Wilk test	W	p	N	a=0,01	a=0,05	test
Heart	Volume	<var>	0.92	0.016	35	normal	not normal	t-test
	Dmean	<var>	0.95	0.04	35	normal	not normal	t-test
	D2cc	<var>	0.97	0.07	50	normal	normal	t-test
	V5Gy [cc]	<var>	0.94	0.02	50	normal	not normal	t-test
Lung L	V5Gy [cc]	<var>	0.97	0.08	50	normal	normal	t-test
	V20Gy [cc]	<var>	0.97	0.05	50	normal	not normal	t-test

APPENDIX III: SUPPLEMENTARY FIGURES

Robustness evaluation 3mm analysis

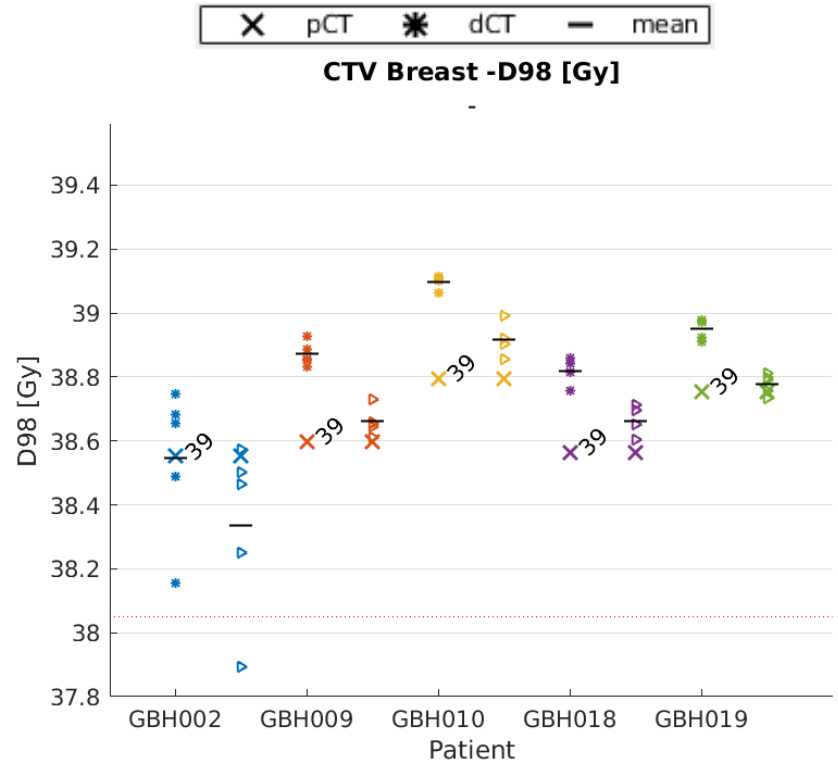

Figure 16: Robustness evaluation of the D98% for the CTV Breast. (red dotted line) represent the clinical goal: D98 >38.05

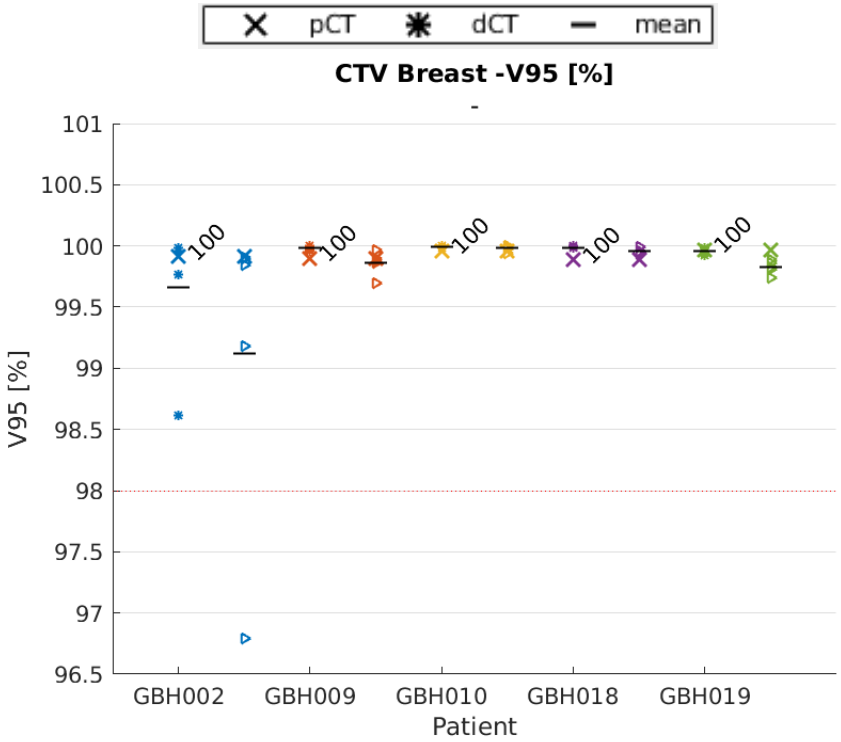

Figure 17: Robustness evaluation of the V95% for the CTV Breast. (red dotted line) represent the clinical goal: D98 >98

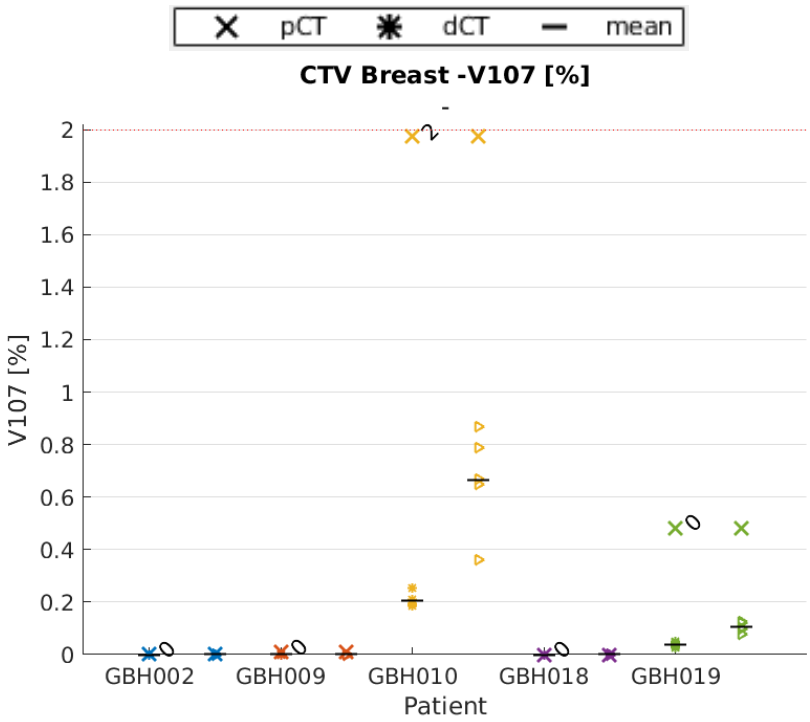

Figure 18: Robustness evaluation of the V107% for the CTV Breast. (red dotted line) represent the clinical goal: V107 <2

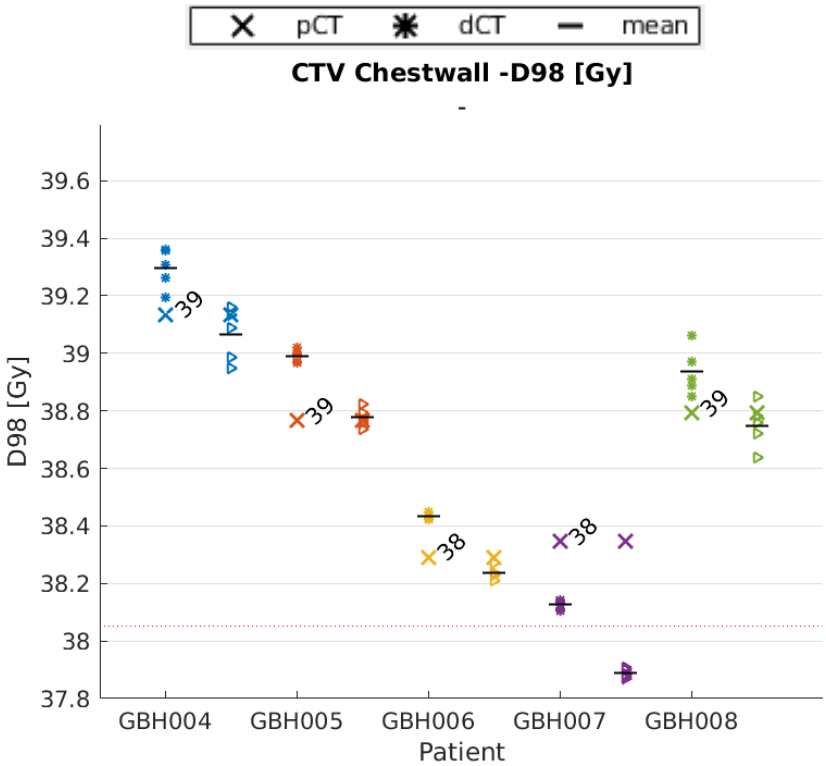

Figure 19: Robustness evaluation of the D98% for the CTV Chestwall. (red dotted line) represent the clinical goal: D98 >38.05

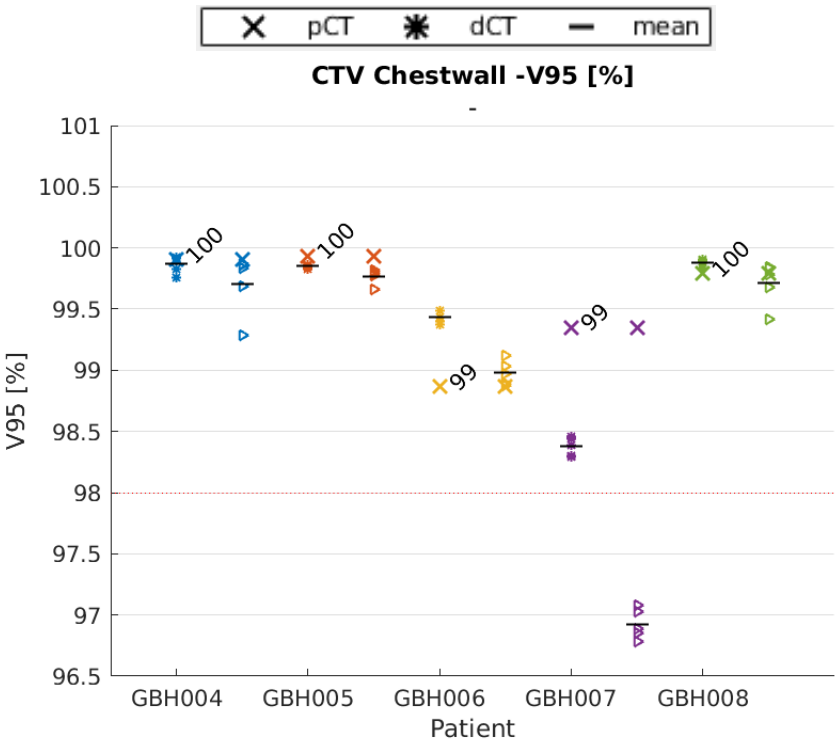

Figure 20: Robustness evaluation of the V95% for the CTV Chestwall. (red dotted line) represent the clinical goal: D98 >98

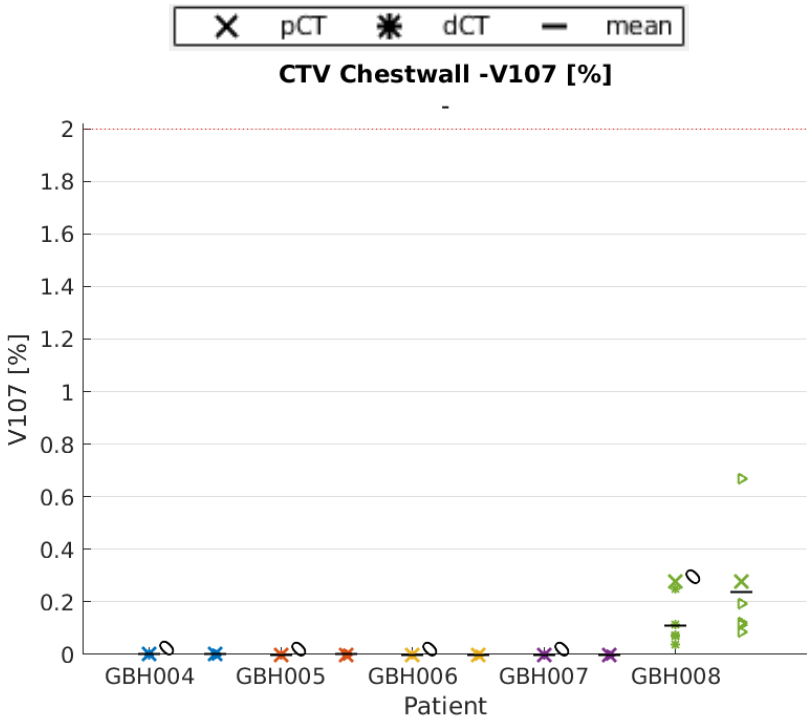

Figure 21: Robustness evaluation of the V107% for the CTV Chestwall. (red dotted line) represent the clinical goal: V107 <2

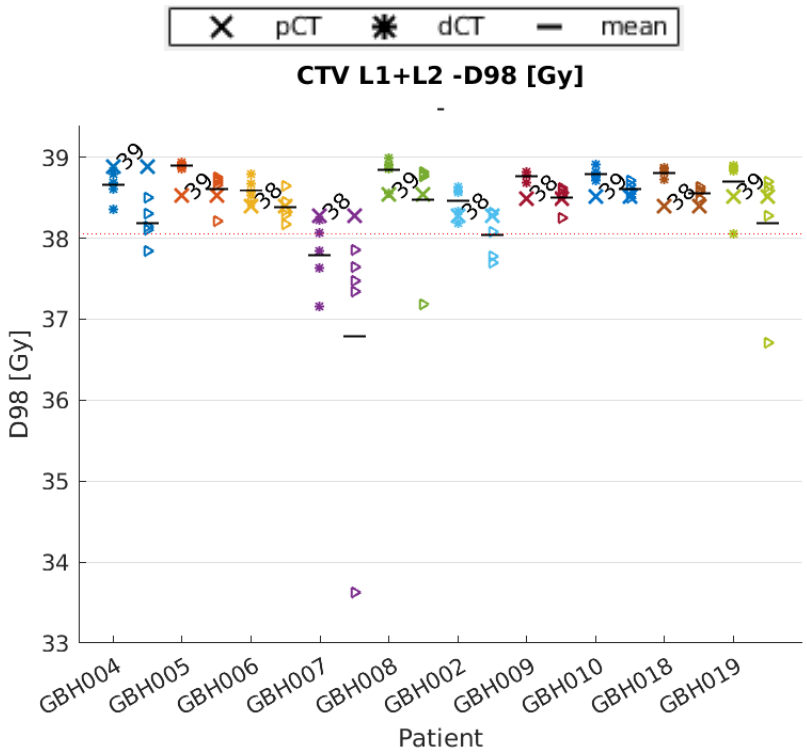

Figure 22: Robustness evaluation of the D98% for the CTV L1+L2. (red dotted line) represent the clinical goal: D98 >38.05

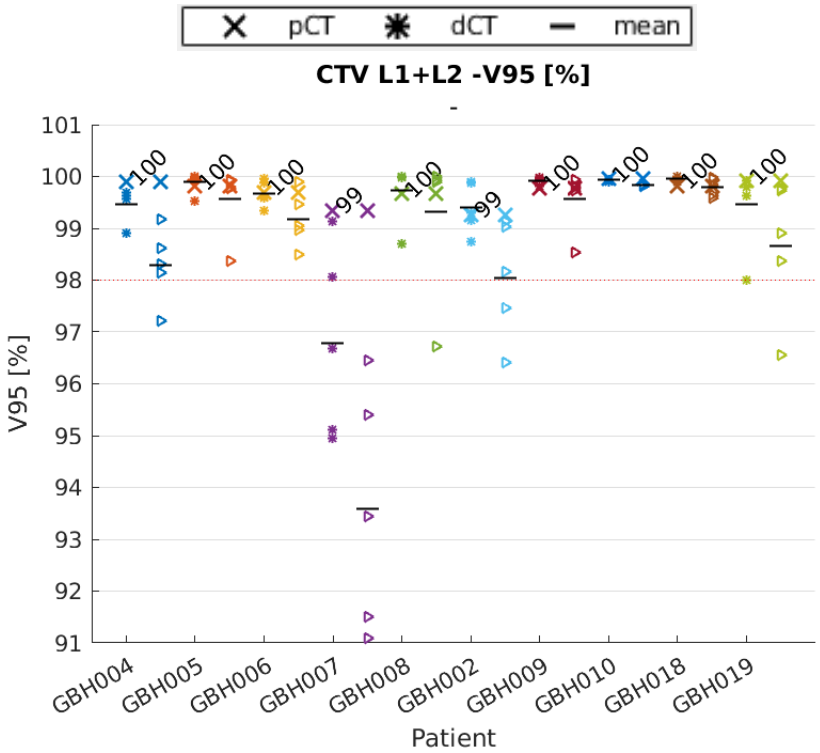

Figure 23: Robustness evaluation of the V95% for the CTV L1+L2. (red dotted line) represent the clinical goal: D98 >98

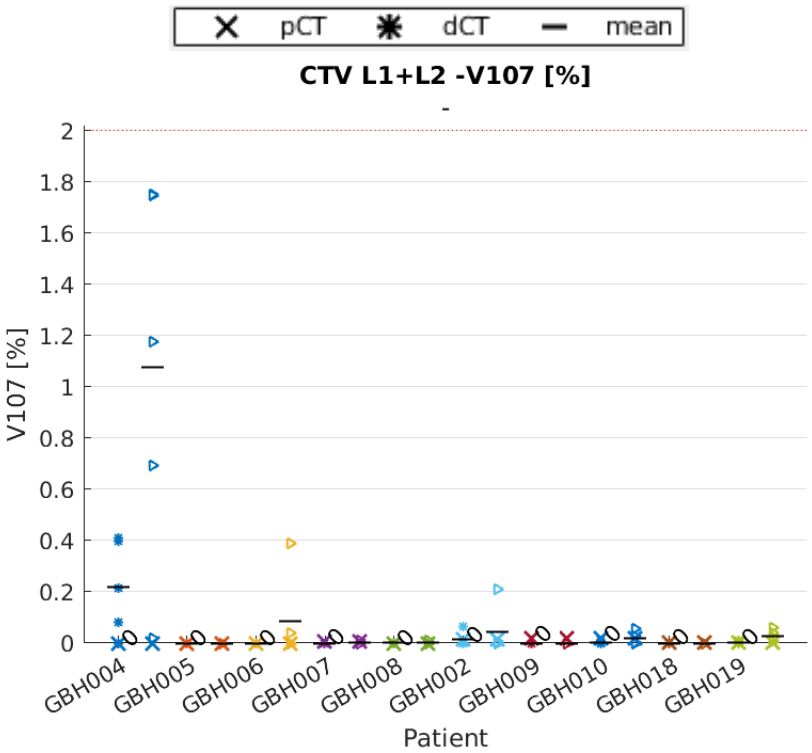

Figure 24: Robustness evaluation of the V107% for the CTV L1+L2. (red dotted line) represent the clinical goal: V107 <2

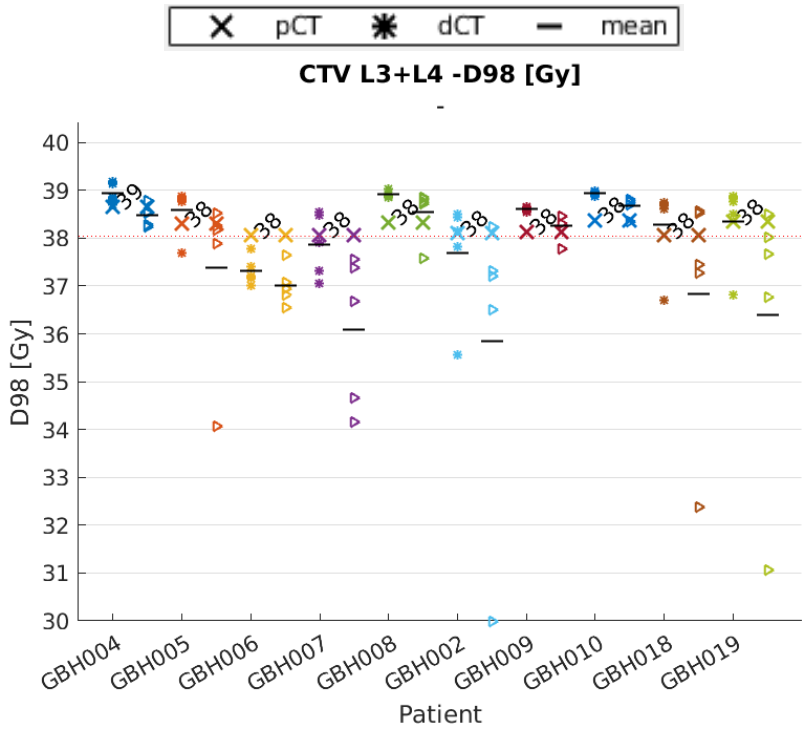

Figure 25: Robustness evaluation of the D98% for the CTV L3+L4. (red dotted line) represent the clinical goal: D98 >38.05

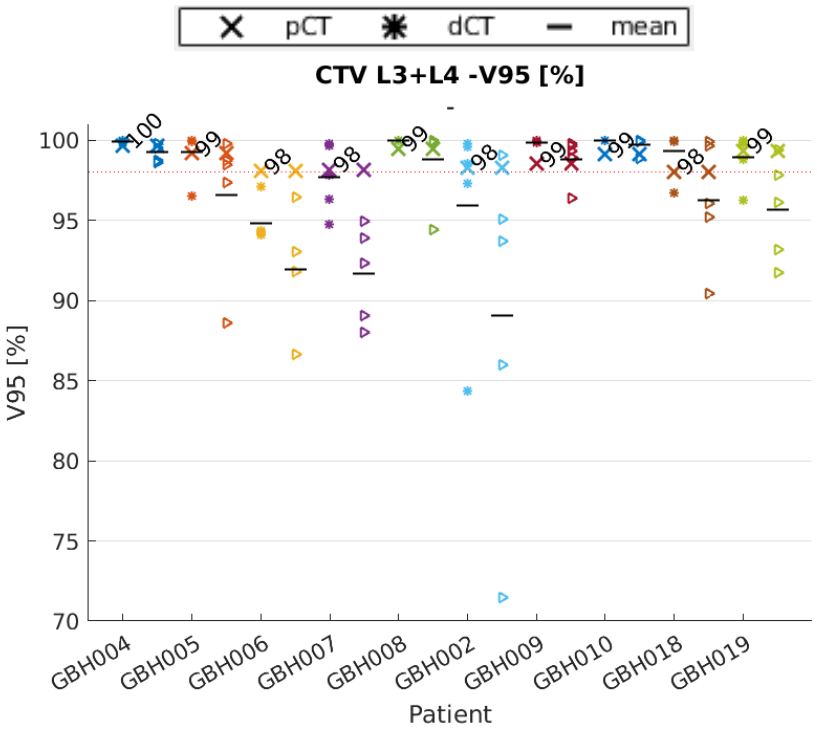

Figure 26: Robustness evaluation of the V95% for the CTV L3+L4. (red dotted line) represent the clinical goal: D98 >98

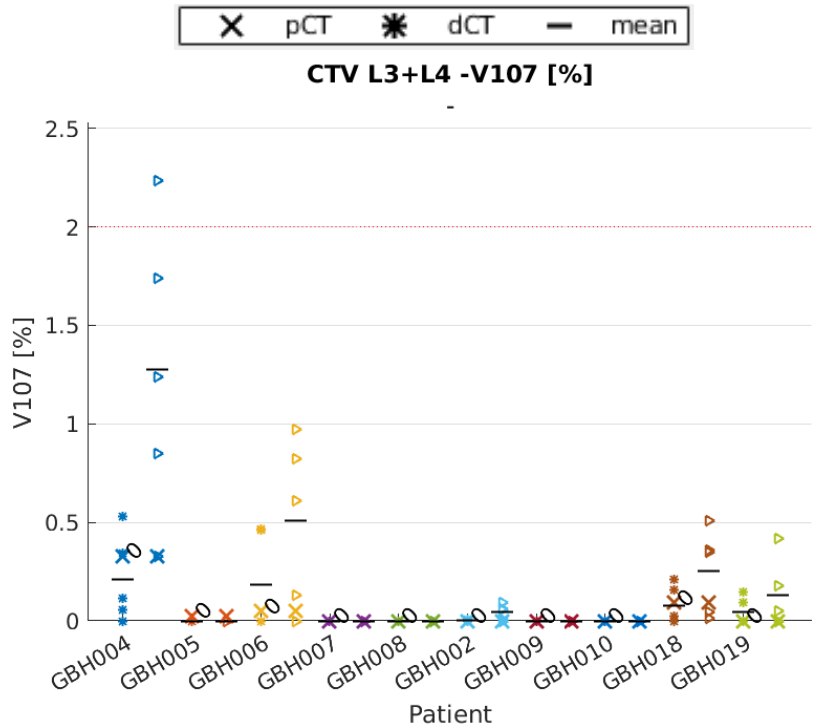

Figure 27: Robustness evaluation of the V107% for the CTV L3+L4. (red dotted line) represent the clinical goal: V107 <2

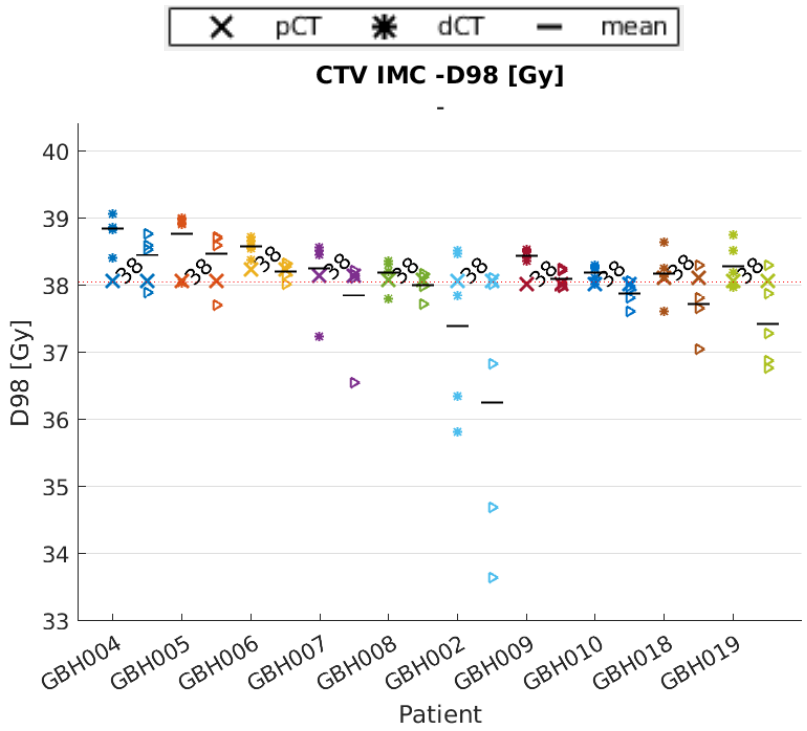

Figure 28: Robustness evaluation of the D98% for the CTV IMC. (red dotted line) represent the clinical goal: D98 >38.05

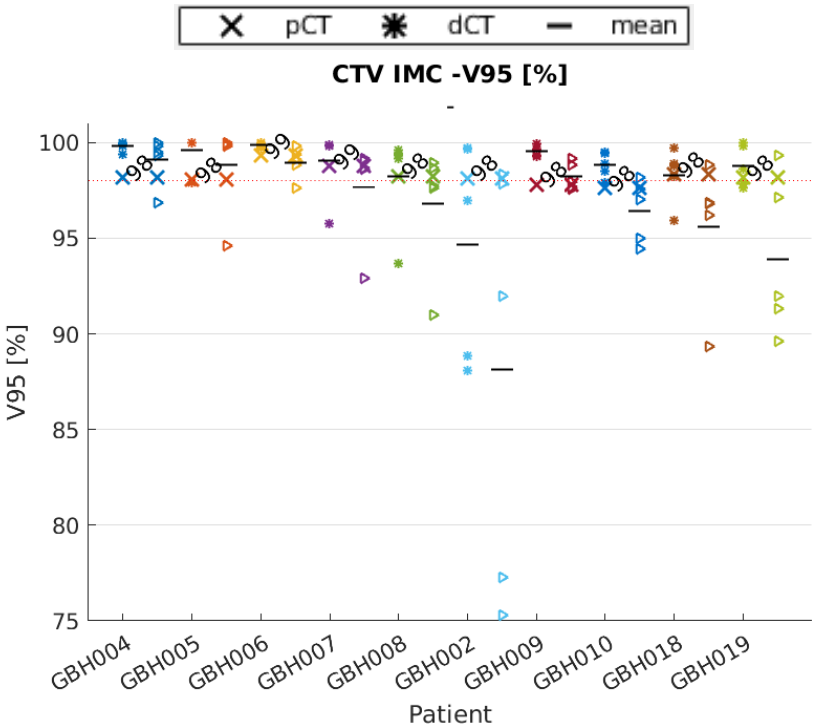

Figure 29: Robustness evaluation of the V95% for the CTV IMC. (red dotted line) represent the clinical goal: D98 >98

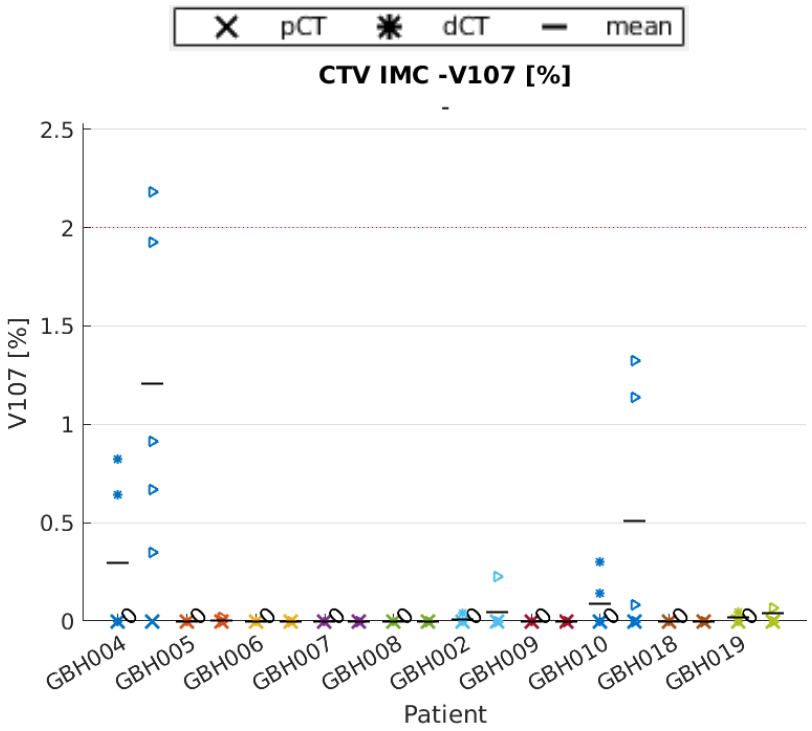

Figure 30: Robustness evaluation of the V107% for the CTV IMC. (red dotted line) represent the clinical goal: V107 <2

QQ-plots and Histograms for normal distribution 1 mm robustness evaluation

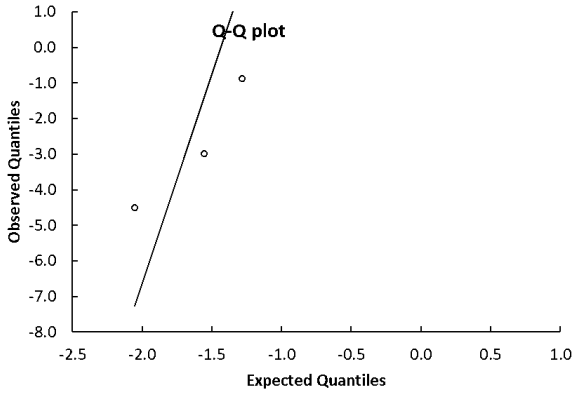

(a) QQ-Plot

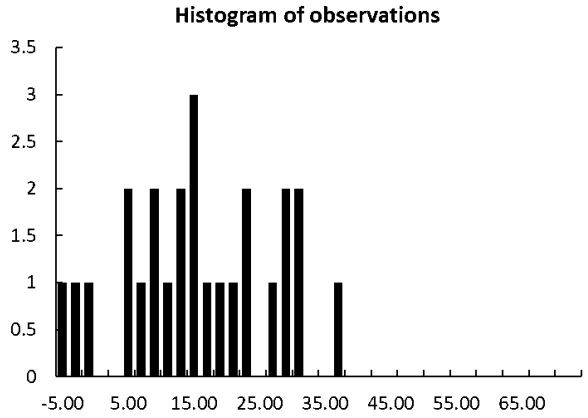

(b) Histogram

Figure 31: Chest wall Volume

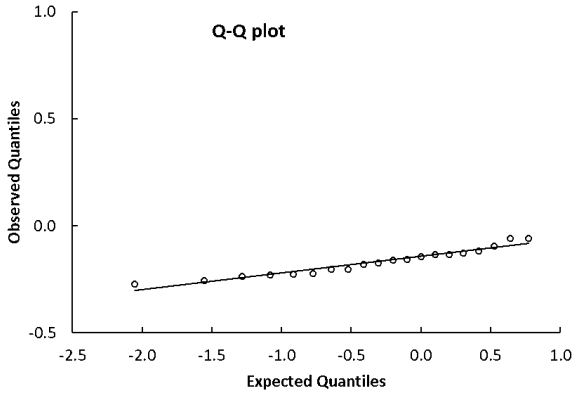

(a) QQ-Plot

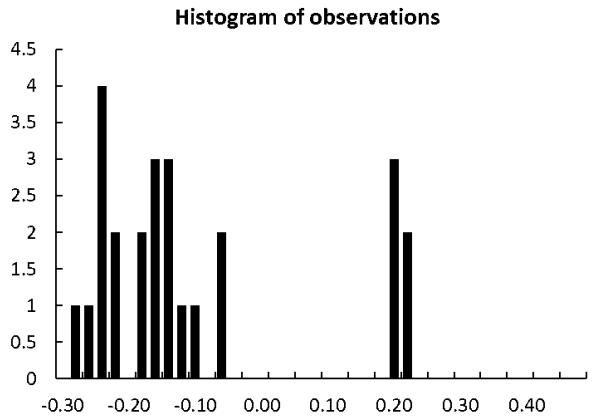

(b) Histogram

Figure 32: Chestwall D98

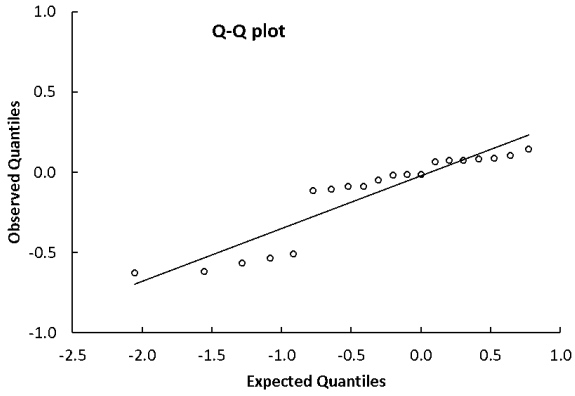

(a) QQ-Plot

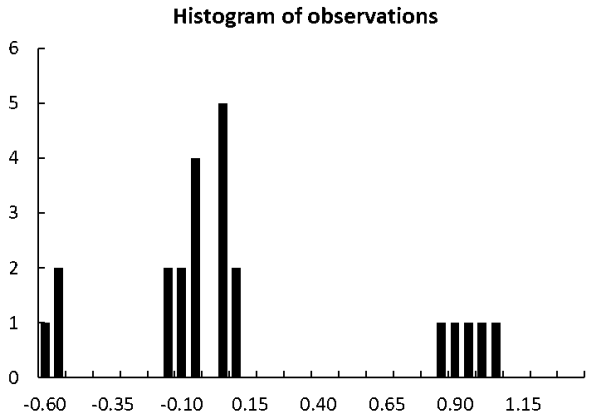

(b) Histogram

Figure 33: Chestwall V95

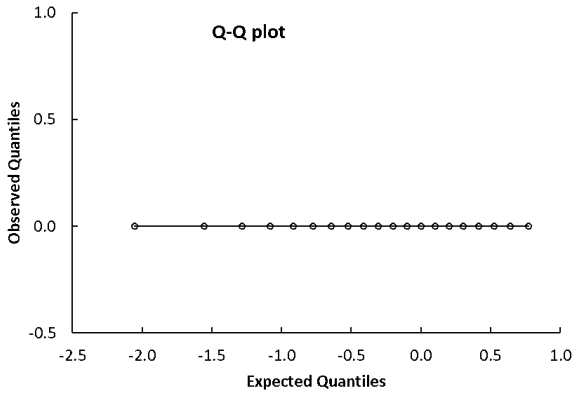

(a) QQ-Plot

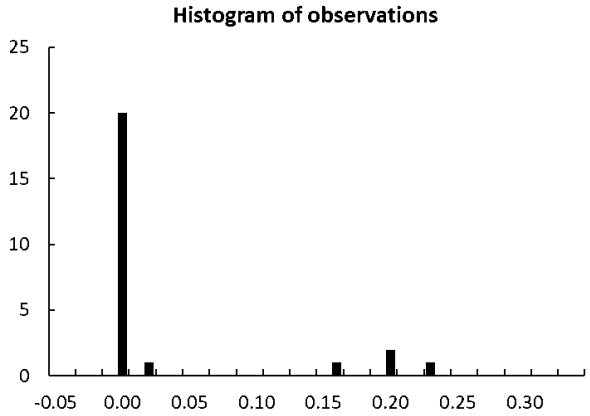

(b) Histogram

Figure 34: Chestwall V107

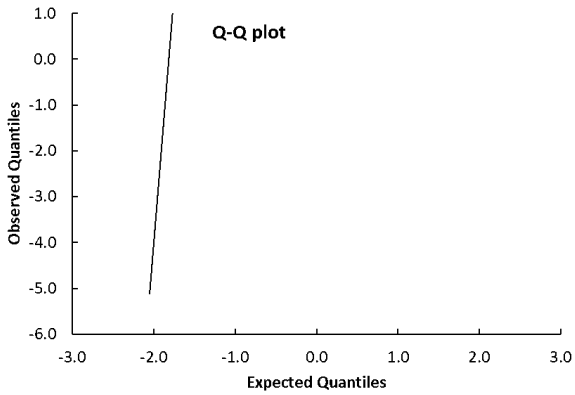

(a) QQ-Plot

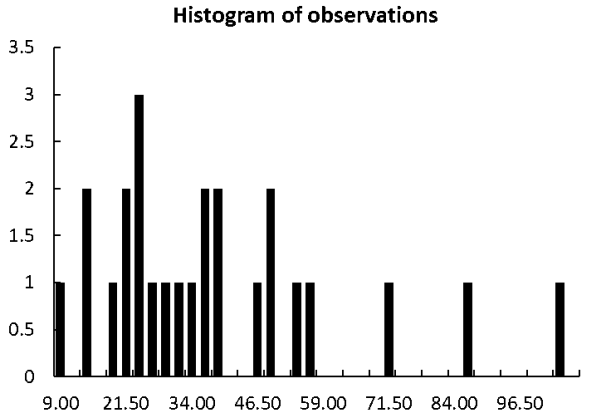

(b) Histogram

Figure 35: Breast Volume

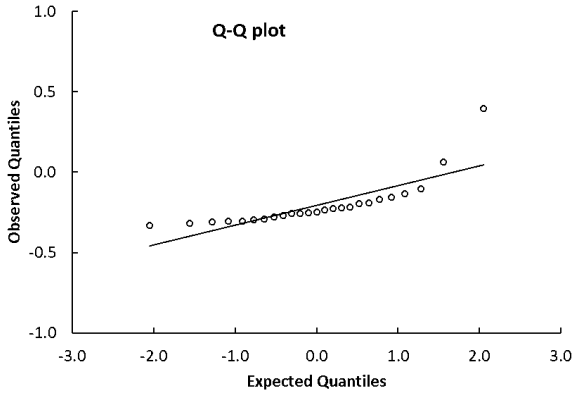

(a) QQ-Plot

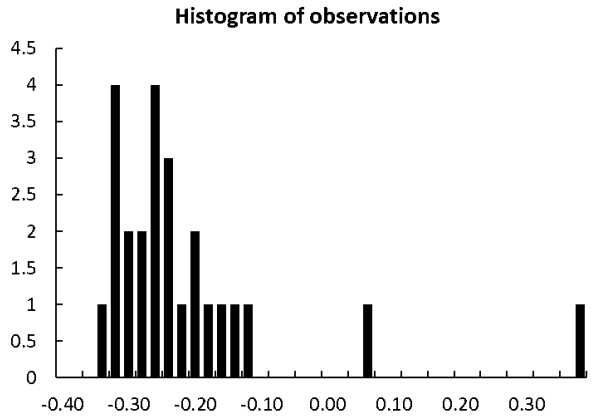

(b) Histogram

Figure 36: Breast D98

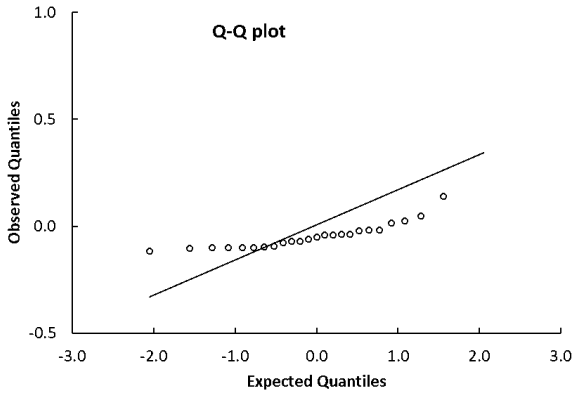

(a) QQ-Plot

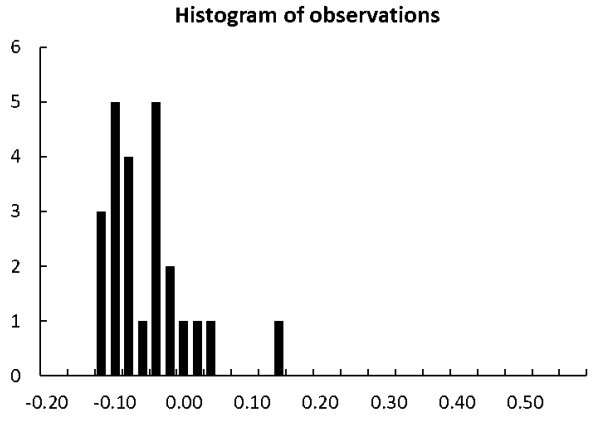

(b) Histogram

Figure 37: Breast V95

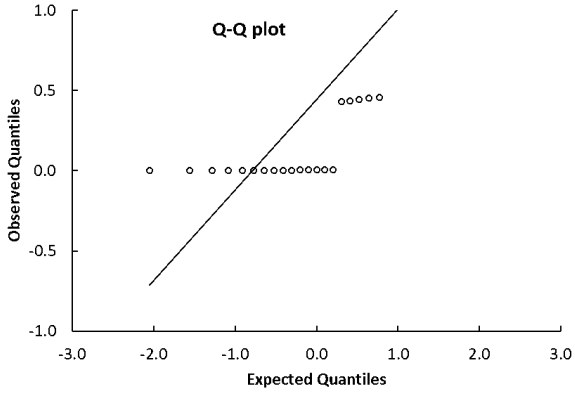

(a) QQ-Plot

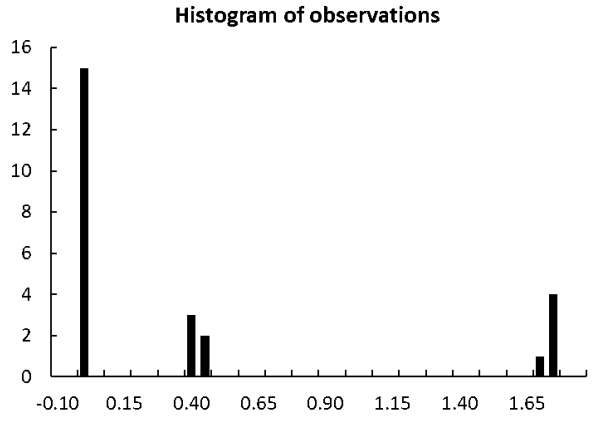

(b) Histogram

Figure 38: Breast V107

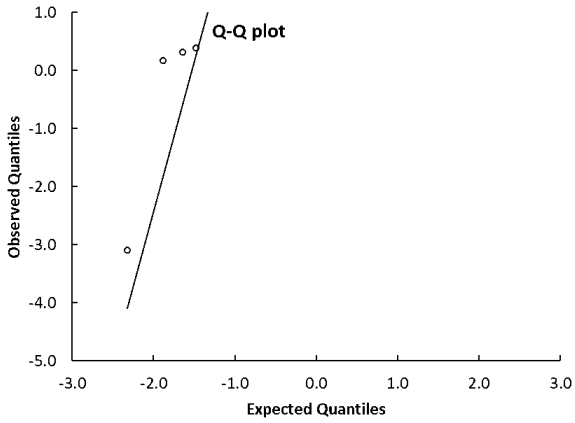

(a) QQ-Plot

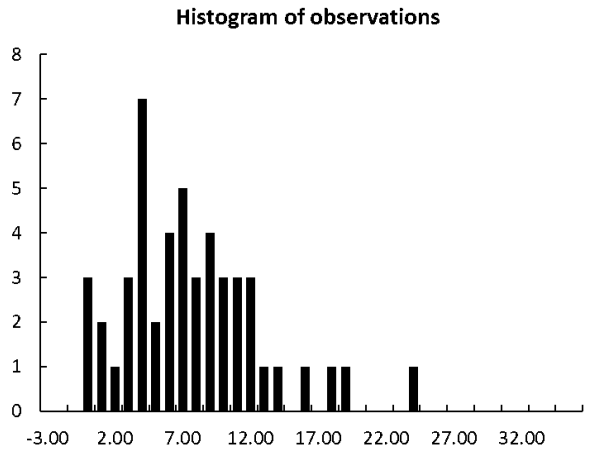

(b) Histogram

Figure 39: L1+L2 Volume

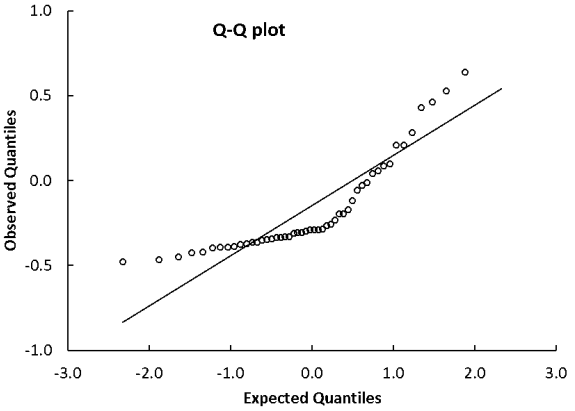

(a) QQ-Plot

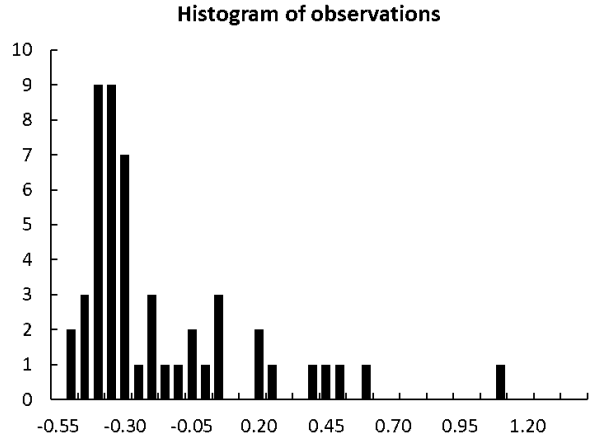

(b) Histogram

Figure 40: L1+L2 D98

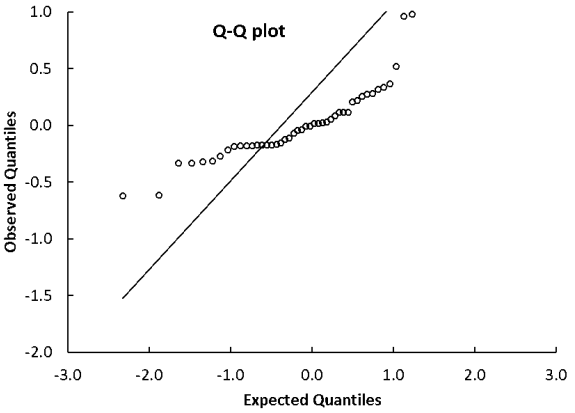

(a) QQ-Plot

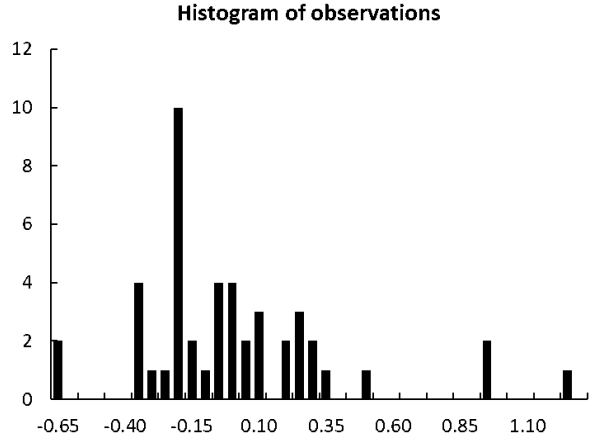

(b) Histogram

Figure 41: L1+L2 V95

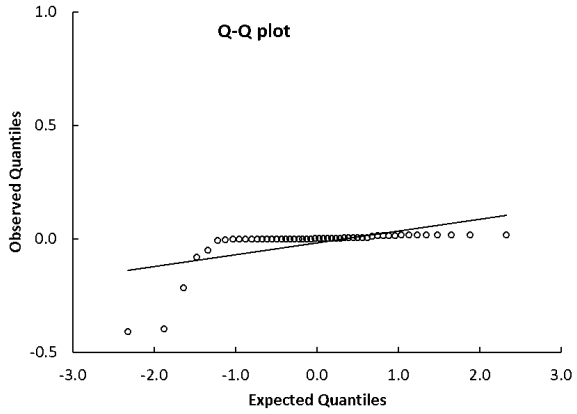

(a) QQ-Plot

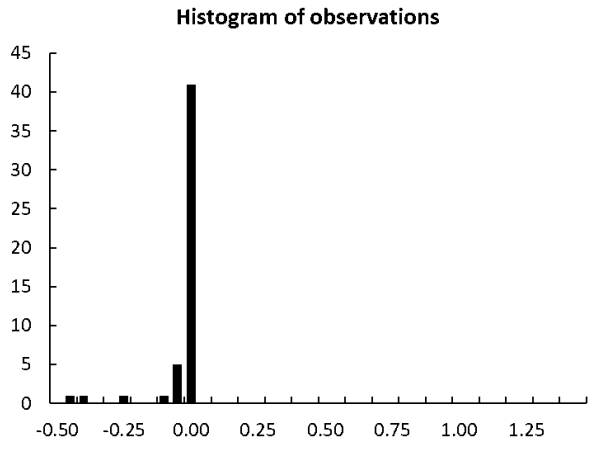

(b) Histogram

Figure 42: L1+L2 V107

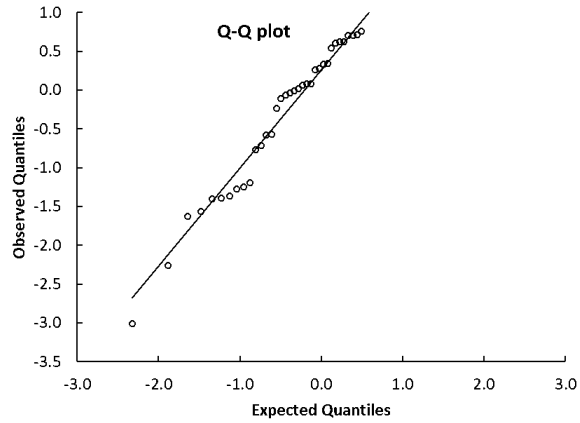

(a) QQ-Plot

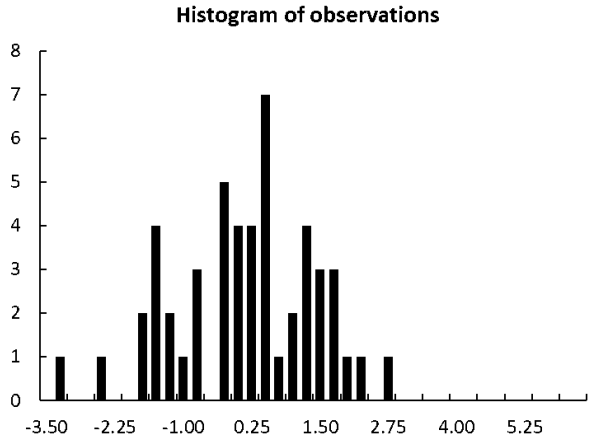

(b) Histogram

Figure 43: L3+L4 Volume

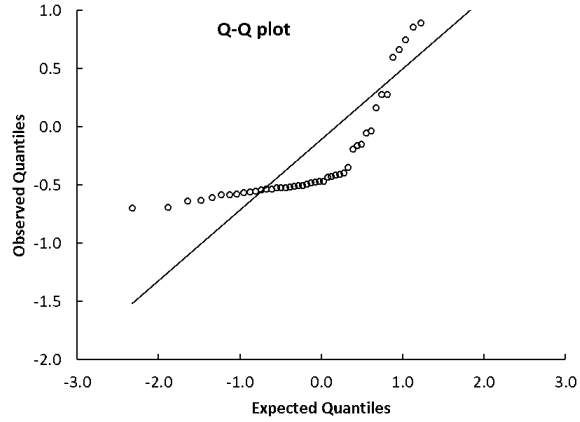

(a) QQ-Plot

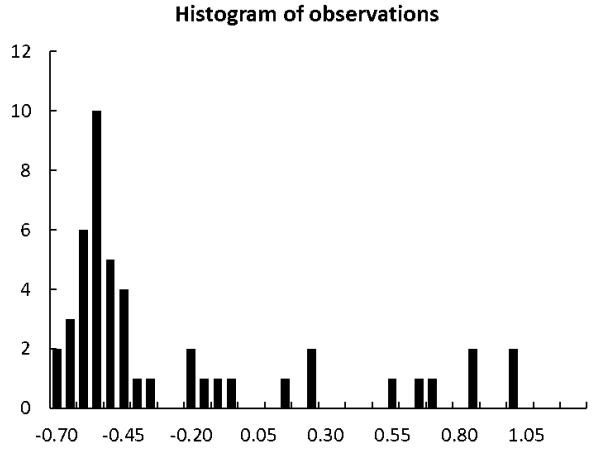

(b) Histogram

Figure 44: L3+L4 D98

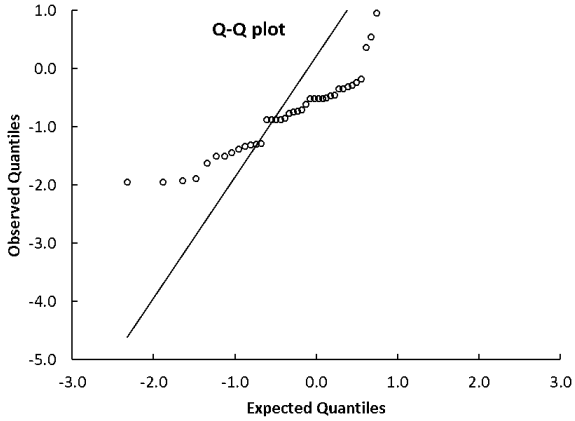

(a) QQ-Plot

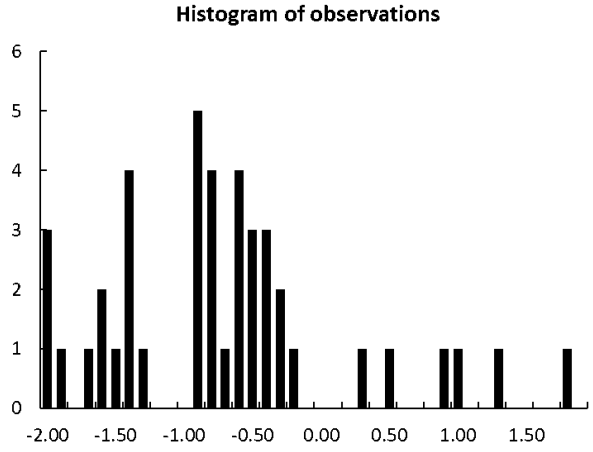

(b) Histogram

Figure 45: L3+L4 V95

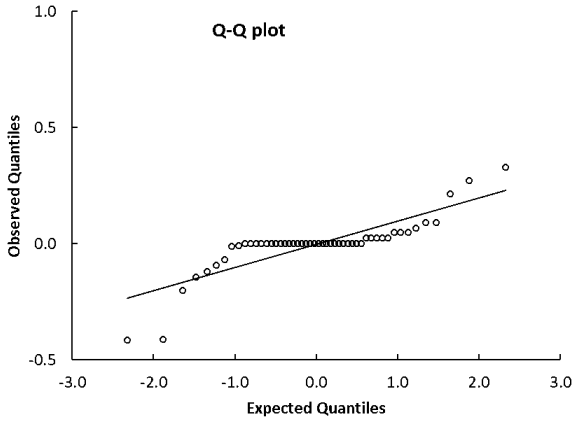

(a) QQ-Plot

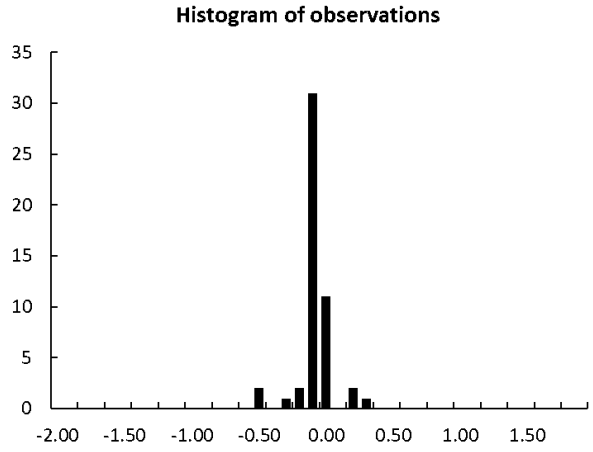

(b) Histogram

Figure 46: L3+L4 V107

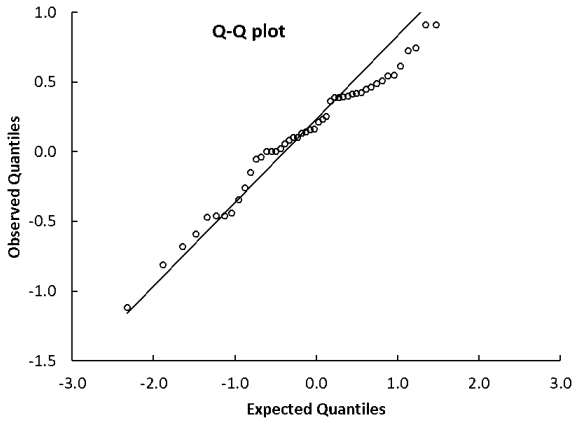

(a) QQ-Plot

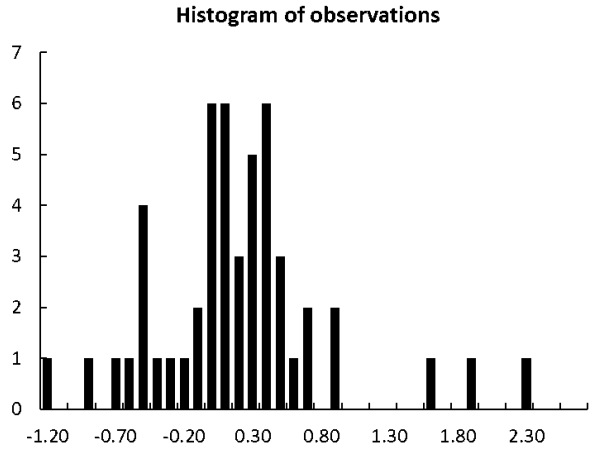

(b) Histogram

Figure 47: IMC Volume

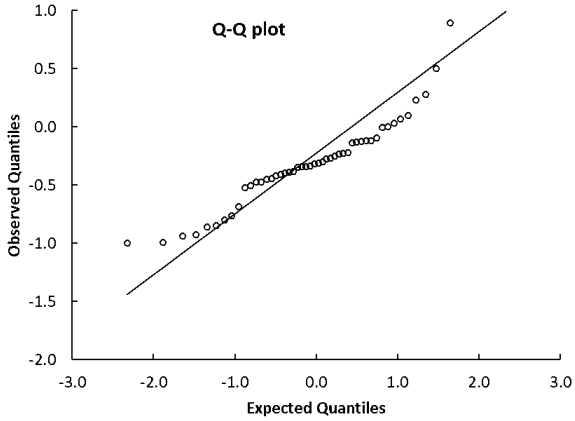

(a) QQ-Plot

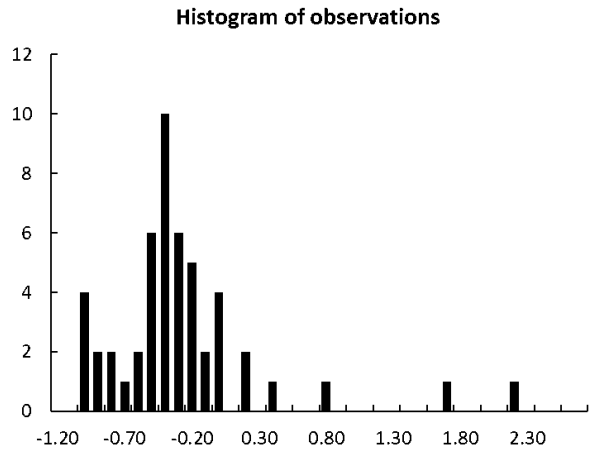

(b) Histogram

Figure 48: IMC D98

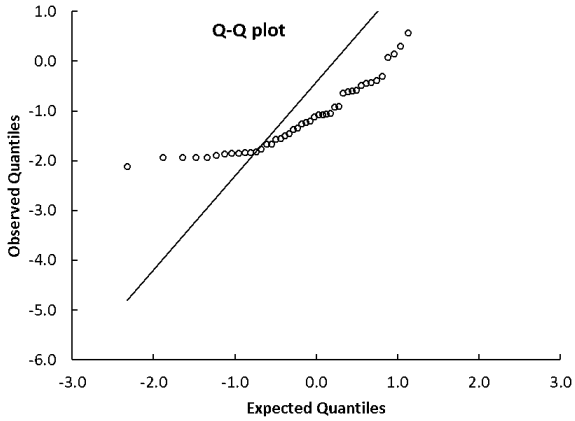

(a) QQ-Plot

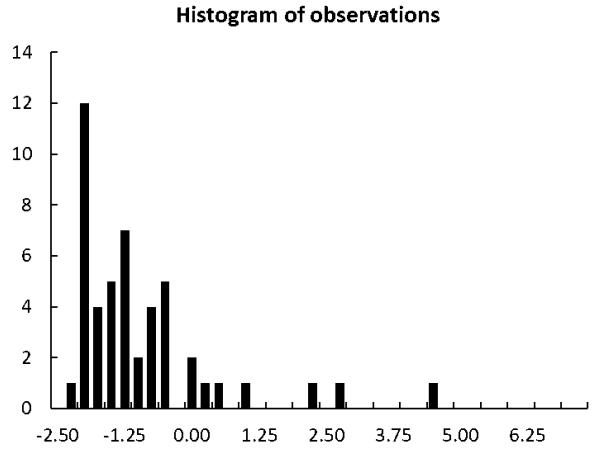

(b) Histogram

Figure 49: IMC V95

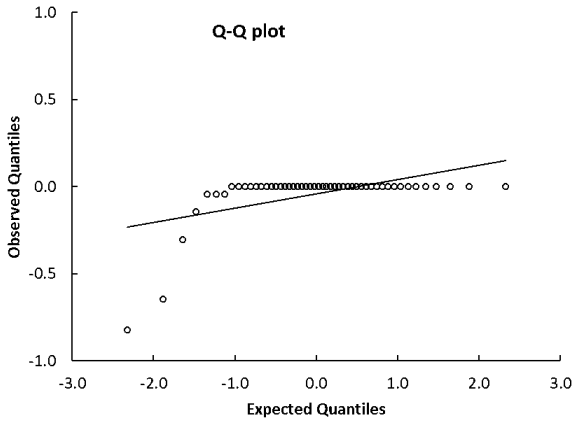

(a) QQ-Plot

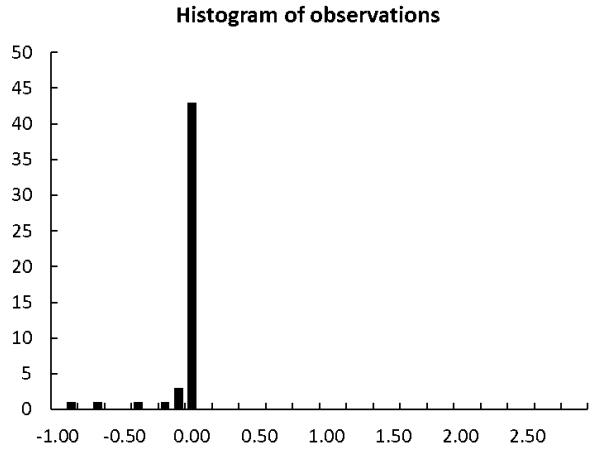

(b) Histogram

Figure 50: IMC V107

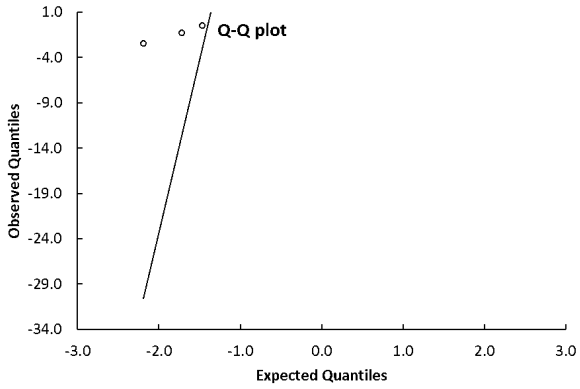

(a) QQ-Plot

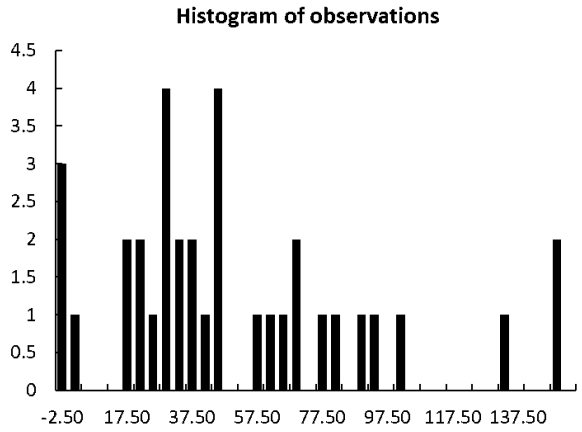

(b) Histogram

Figure 51: Heart Volume

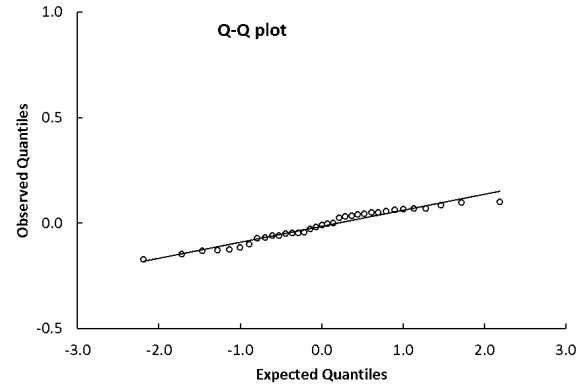

(a) QQ-Plot

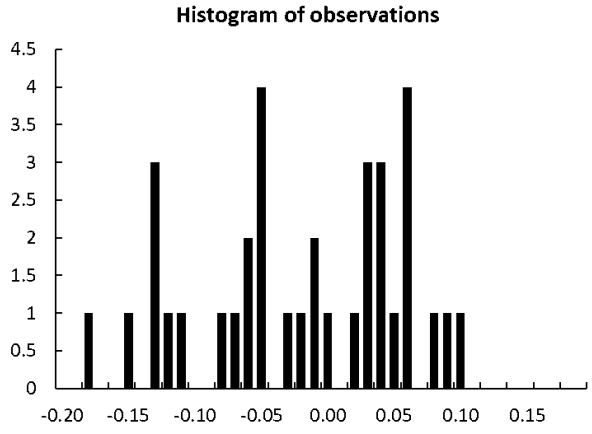

(b) Histogram

Figure 52: Heart Dmean

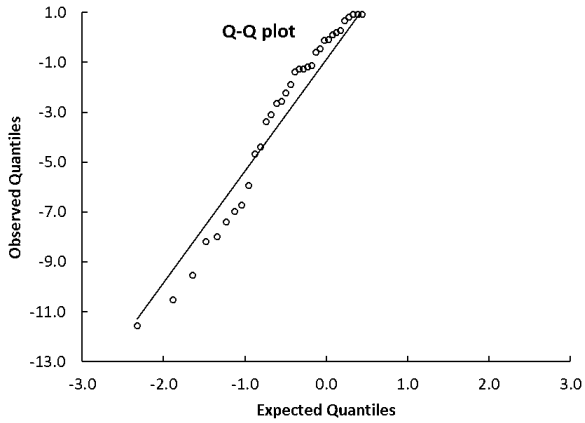

(a) QQ-Plot

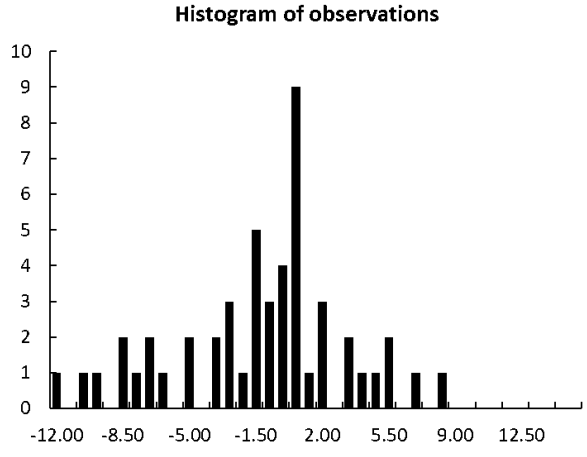

(b) Histogram

Figure 53: Heart D2cc

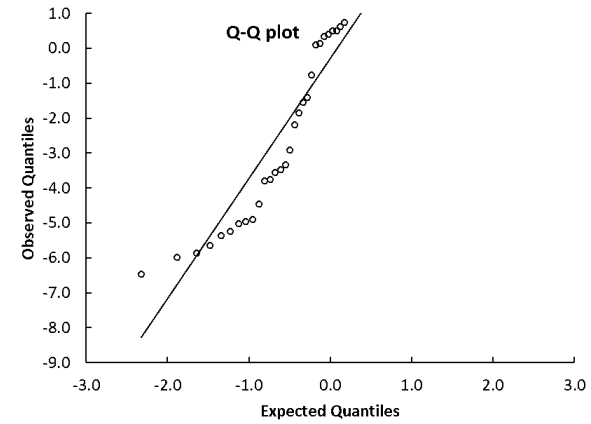

(a) QQ-Plot

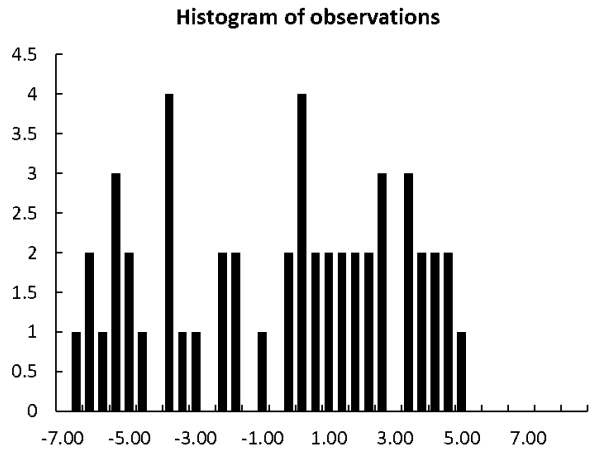

(b) Histogram

Figure 54: Heart V5Gy

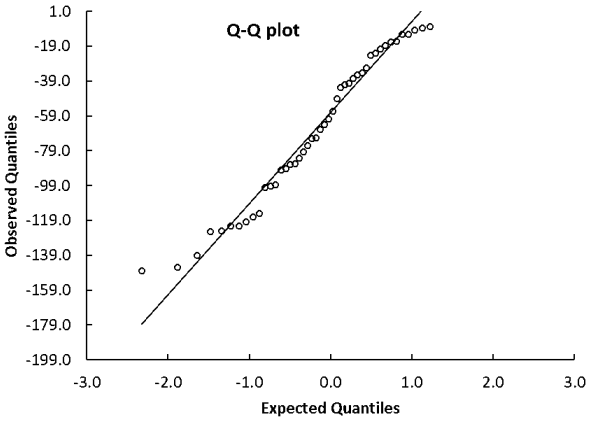

(a) QQ-Plot

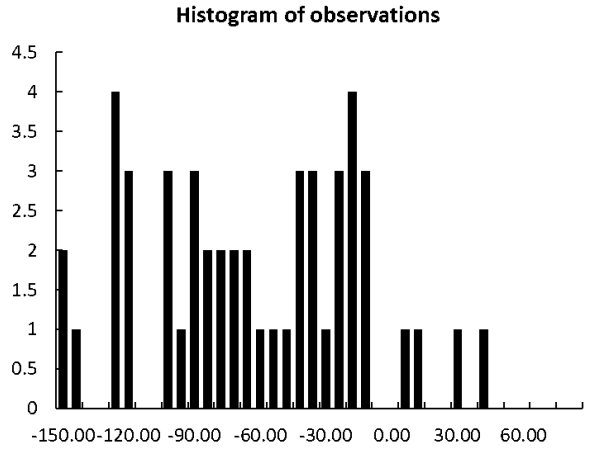

(b) Histogram

Figure 55: Left lung V5Gy

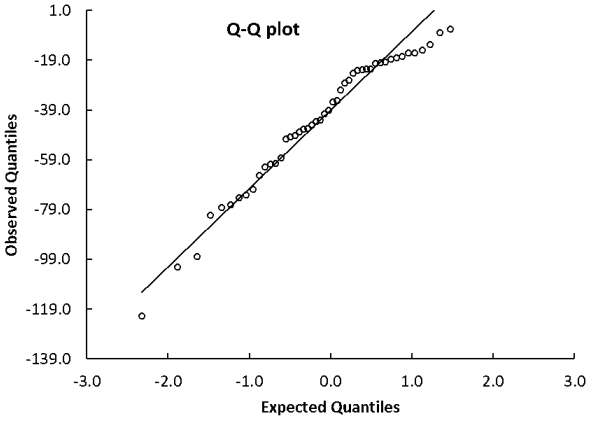

(a) QQ-Plot

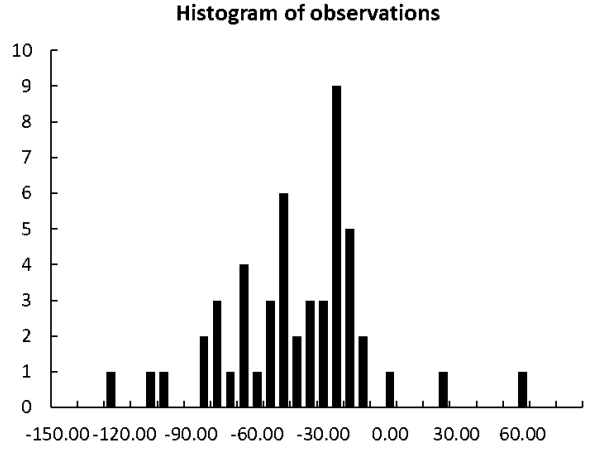

(b) Histogram

Figure 56: Left lung V20Gy

QQ Plots and Histograms for normal distribution 3 mm robustness evaluation

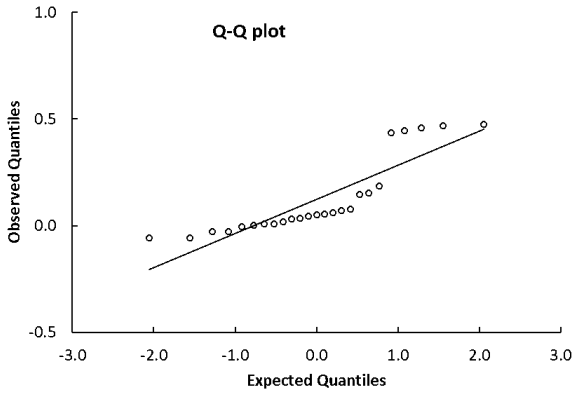

(a) QQ-Plot

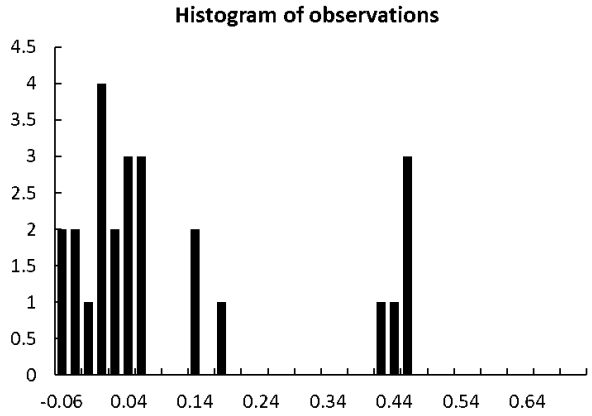

(b) Histogram

Figure 57: Chest wall D98 3mm

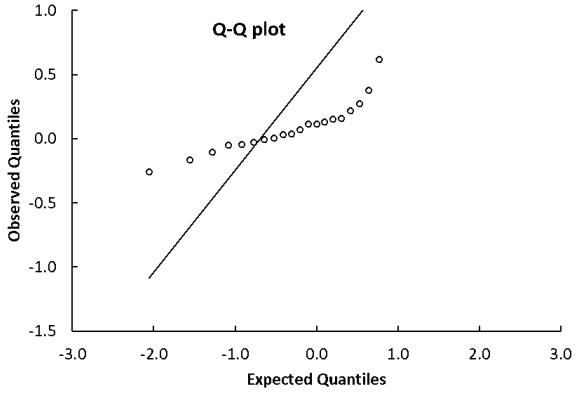

(a) QQ-Plot

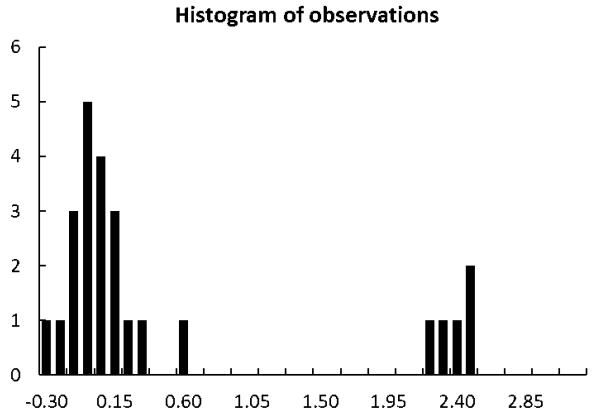

(b) Histogram

Figure 58: Chest wall V95 3mm

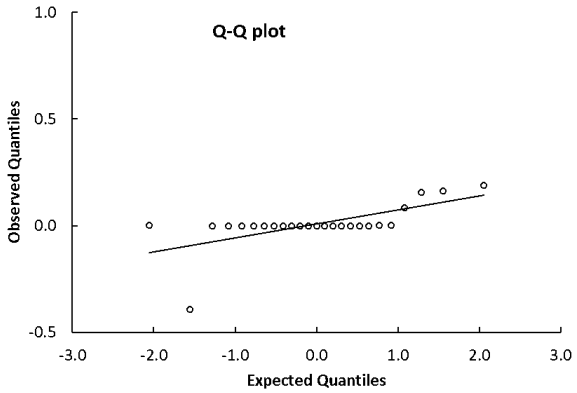

(a) QQ-Plot

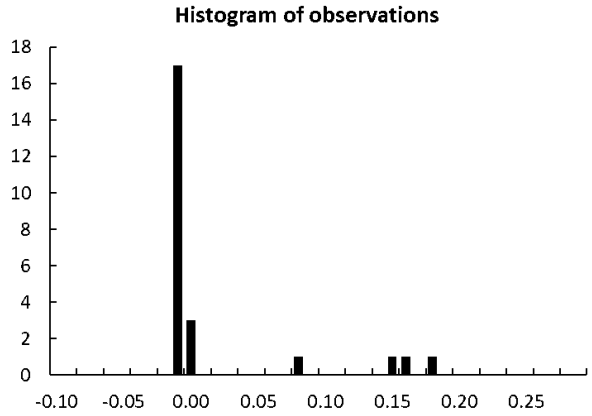

(b) Histogram

Figure 59: Chest wall V107 3mm

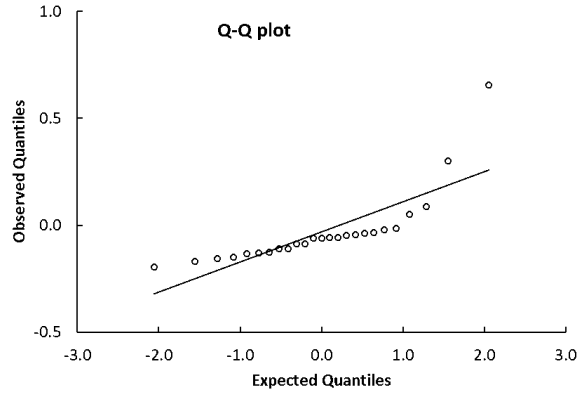

(a) QQ-Plot

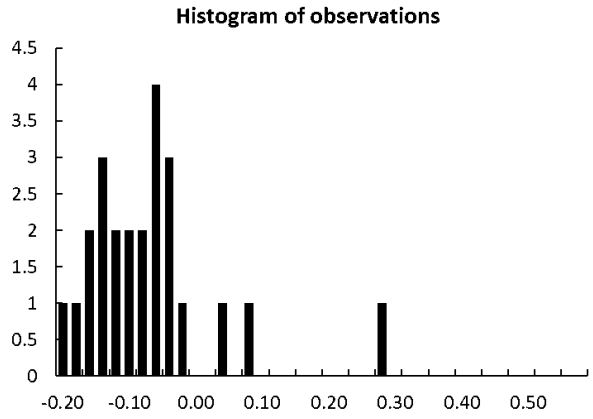

(b) Histogram

Figure 60: Chest wall D98 3mm

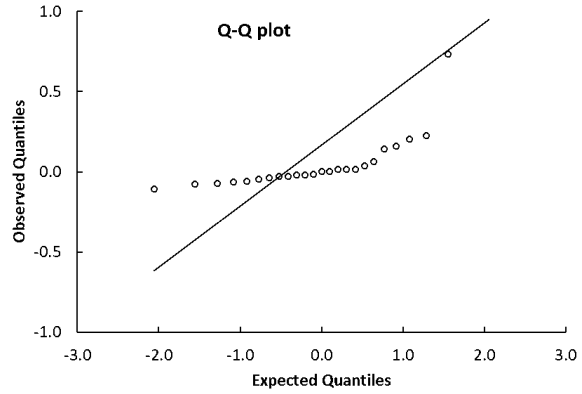

(a) QQ-Plot

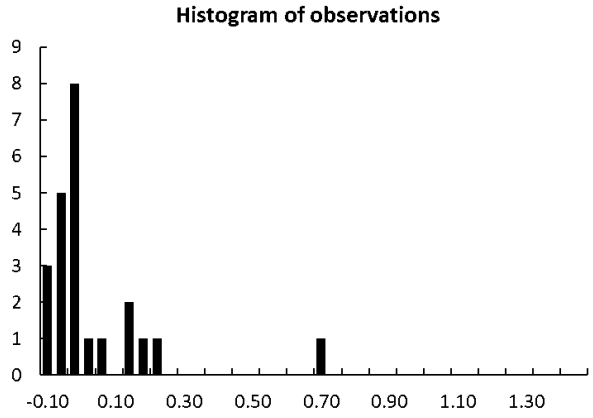

(b) Histogram

Figure 61: Chest wall V95 3mm

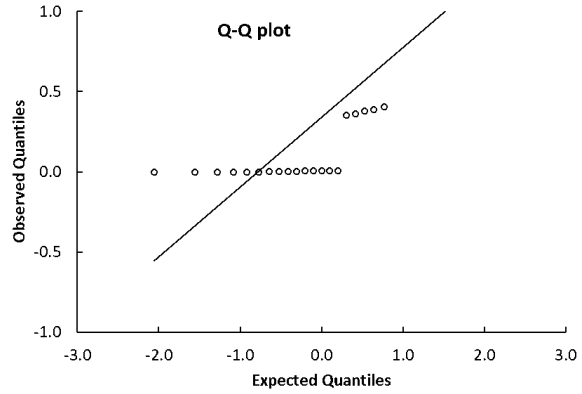

(a) QQ-Plot

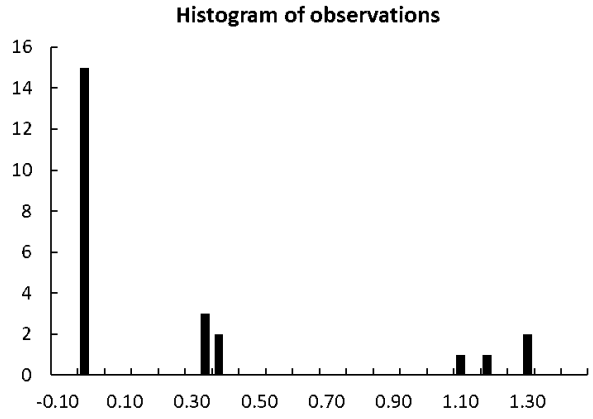

(b) Histogram

Figure 62: Chest wall V107 3mm

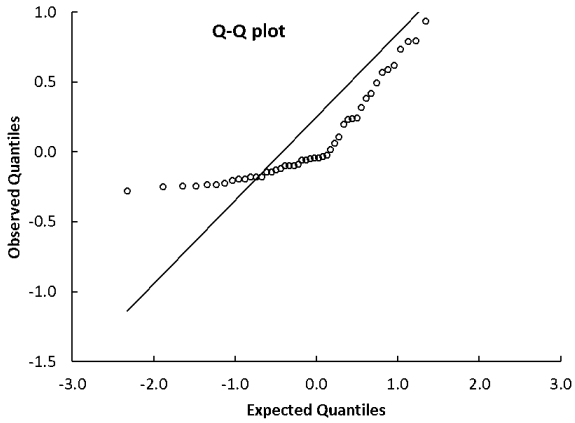

(a) QQ-Plot

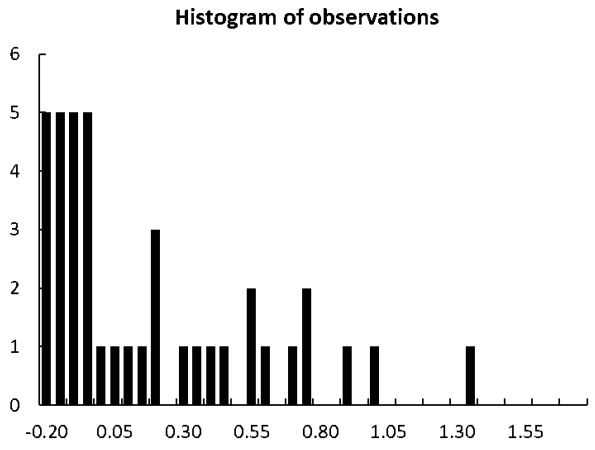

(b) Histogram

Figure 63: Chest wall D98 3mm

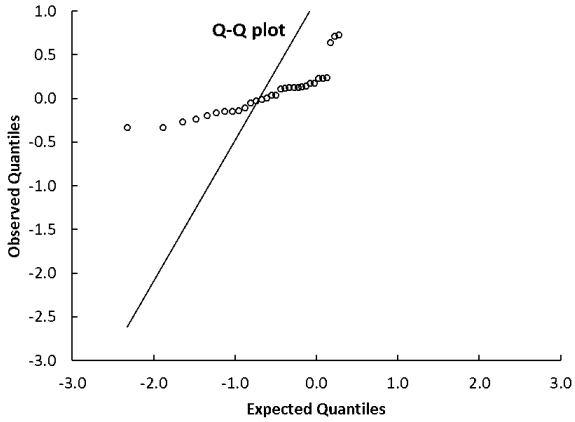

(a) QQ-Plot

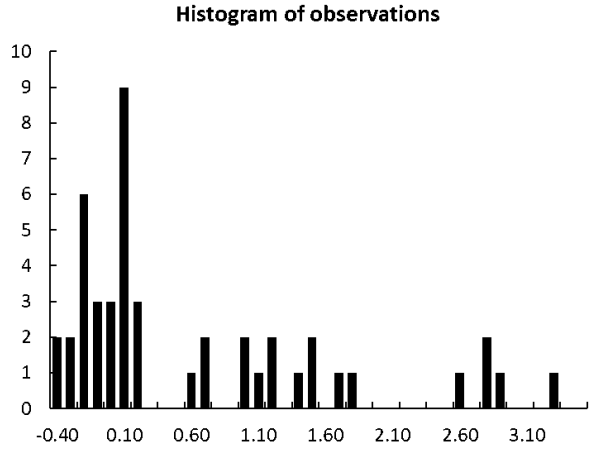

(b) Histogram

Figure 64: Chest wall V95 3mm

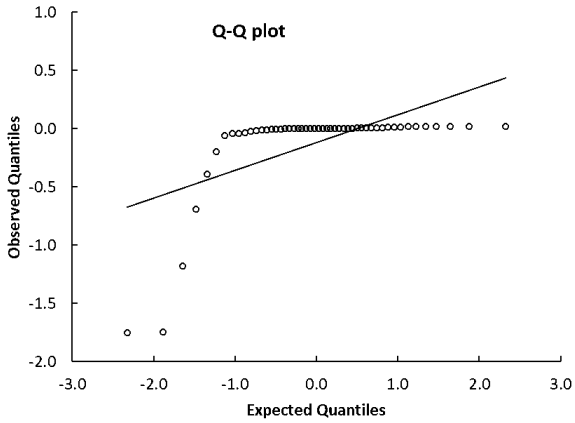

(a) QQ-Plot

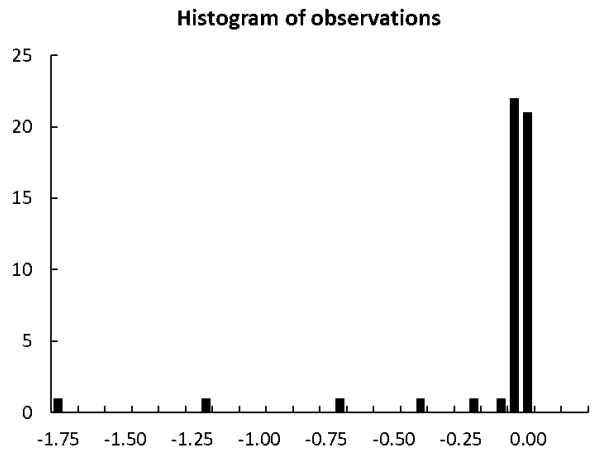

(b) Histogram

Figure 65: Chest wall V107 3mm

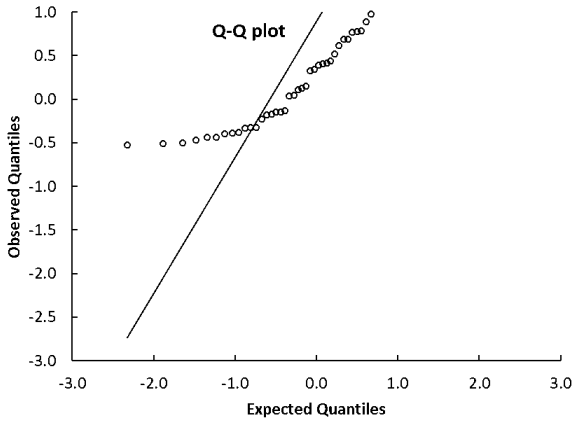

(a) QQ-Plot

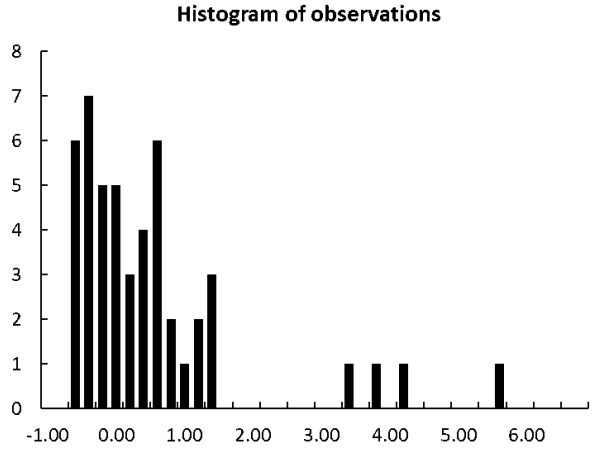

(b) Histogram

Figure 66: Chest wall D98 3mm

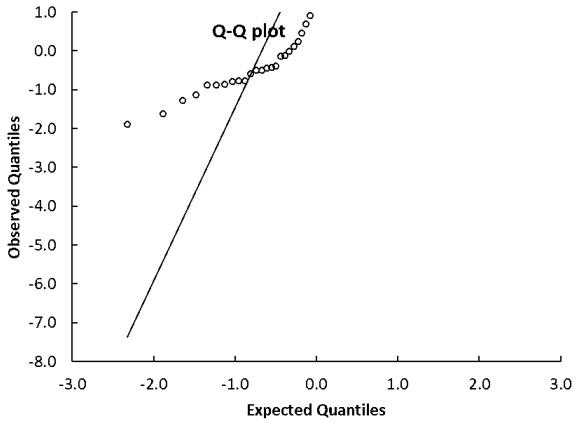

(a) QQ-Plot

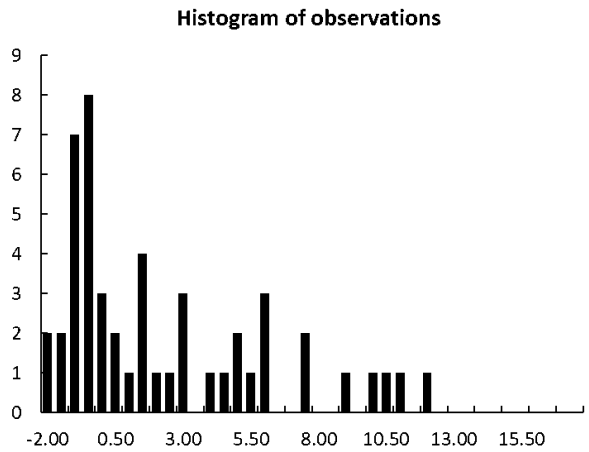

(b) Histogram

Figure 67: Chest wall V95 3mm

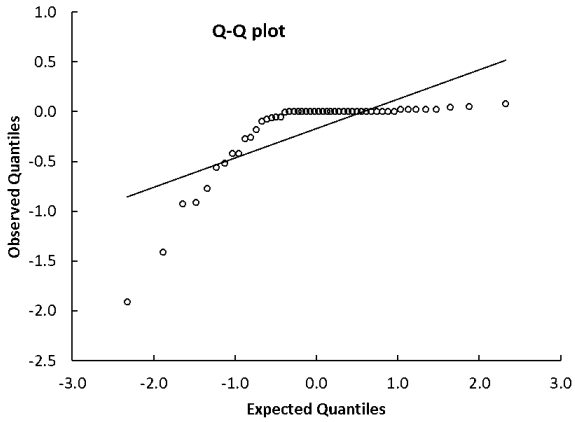

(a) QQ-Plot

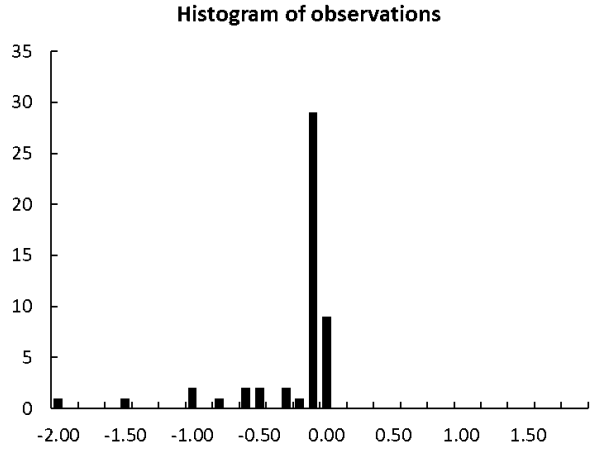

(b) Histogram

Figure 68: Chest wall V107 3mm

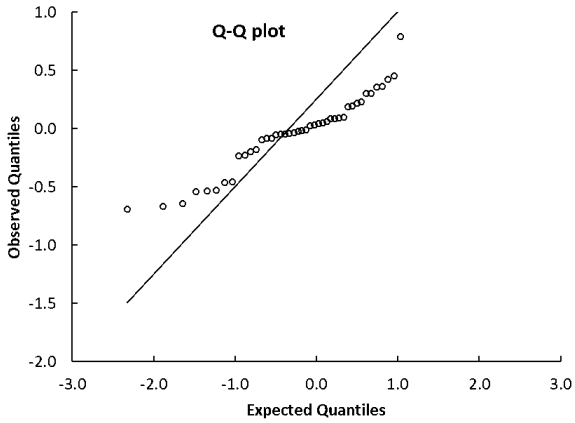

(a) QQ-Plot

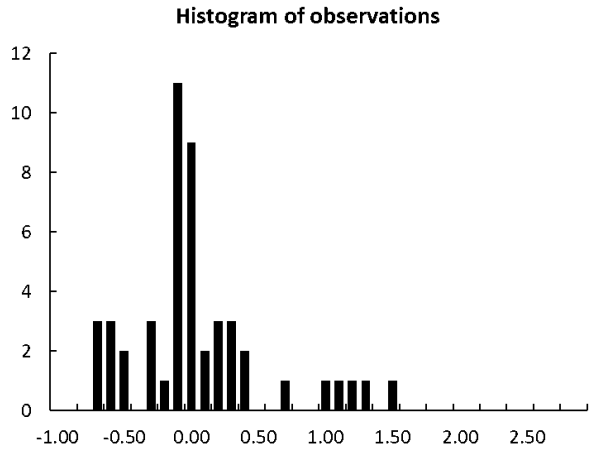

(b) Histogram

Figure 69: Chest wall D98 3mm

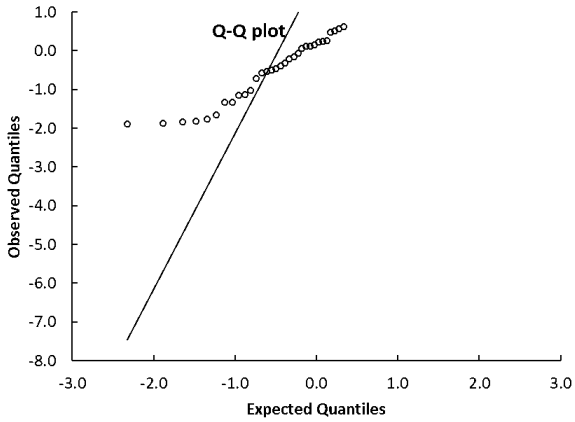

(a) QQ-Plot

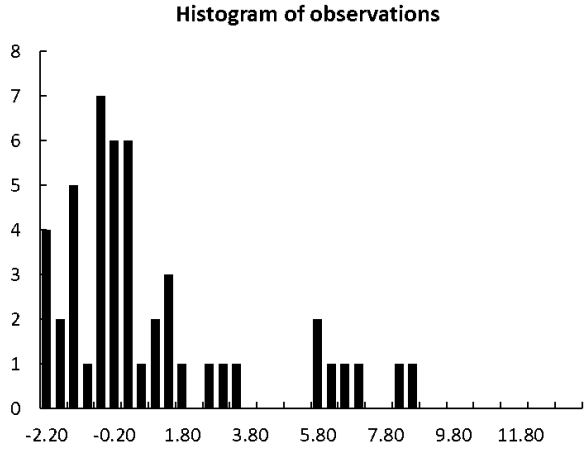

(b) Histogram

Figure 70: Chest wall V95 3mm

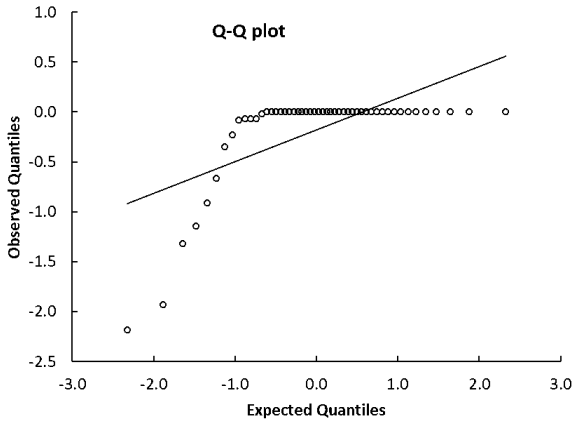

(a) QQ-Plot

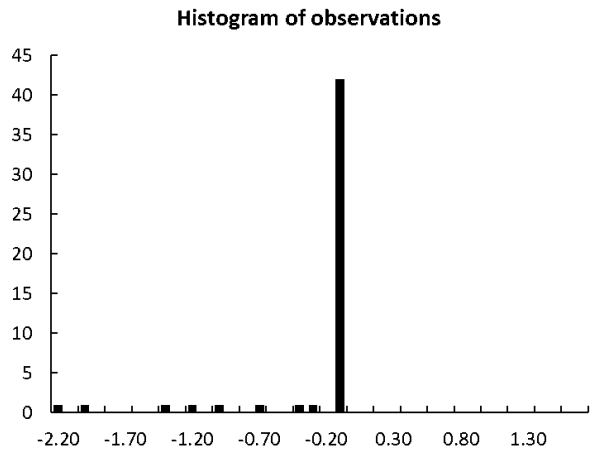

(b) Histogram

Figure 71: Chest wall V107 3mm